Institute of Solid State Physics
University of Latvia

ANNUAL REPORT 2017

Riga 2018

Annual Report 2017, Institute of Solid State Physics, University of Latvia.
Editor: A.Kuzmins.
Set up at the Institute of Solid State Physics, University of Latvia, Kengaraga Str. 8, LV-1063 Riga, Latvia.

Riga, Institute of Solid State Physics, University of Latvia, 2017, p.43

Director: **Dr. phys. M.Rutkis**
Institute of Solid State Physics, University of Latvia
Kengaraga Str. 8, LV-1063 Riga, Latvia
***Tel.:** +371 67187816*
***Fax:** +371 67132778*
ISSP@cfi.lu.lv
http://www.cfi.lu.lv

Contents

Introduction

The research in solid state physics at the University of Latvia restarted after World War II. The Institute of Solid State Physics (ISSP) of the University of Latvia was established on the basis of Laboratory of Semiconductor Research and Laboratory of Ferro- and Piezoelectric Research in 1978. Since 1986 the ISSP has the status of an independent organization of the University and now is the main material science institute in Latvia.

Four laboratories from the Institute of Physics of the Latvian Academy of Sciences joined our Institute in 1995. Twenty scientists of the former Nuclear Research Centre joined the ISSP in 1999 and established Laboratory of Radiation Physics. In 2004 scientists from the Institute of Physical Energetics joined ISSP and established Laboratory of Organic Materials (Table 1).

In mid 90-ties the ISSP has intensified its teaching activities. A number of researchers have been elected as professors of the University of Latvia. Post-graduate and graduate curricula were offered in solid state physics, material physics, chemical physics, physics of condensed matter, semiconductor physics, and experimental methods and instruments. In 2002 the Chair of Solid State and Material Physics University of Latvia was established at ISSP.

Research and training in optometry and vision science is taking place in the Laboratory of Visual Perception of the ISSP since 1992. Co-located with the Institute, the Optometry Centre has been established in 1995 with facilities for primary eye care and serving as a technological research basis for students and staff.

In December 2000 the ISSP was awarded the **Centre of Excellence of the European Commission** (Centre of Excellence for Advanced Material Research and Technologies – **CAMART**). This honorary recognition with the accompanying financial support of 0.7 M EUR has increased our research activities, particularly extending the list of our research partners and scientists who come to work to our Institute from the leading European research centres.

Next step of CAMART was in 2015, when ISSP won Horizon 2020 Teaming project: "**The Excellence Centre of Advanced Material Research and Technology Transfer – CAMART^2**". 169 proposals were submitted, however only 31 were selected to develop their Business Plans. Between them with a score 14.5 (from 15) was the only project from Latvia submitted by the ISSP in cooperation with Swedish colleagues from the Royal Institute of Technology (KTH) and

Acreo Swedish ICT. During 12 months of the Phase 1 a Business Plan for the future Centre of Excellence CAMART^2 was elaborated, demonstrating the long - term science and innovation development strategy.

The Business Plan was highly estimated in the second phase of Horizon 2020 Teaming project dedicated to the establishment of significantly stronger Centre of Excellence during 2017 – 2023.

The research at the ISSP puts emphasis on four priority directions:

- Functional materials for electronics and photonics,
- Nanotechnology, nanocomposites and ceramics,
- Thin films and coating technologies,
- Theoretical and experimental studies of materials structure and properties.

The highest decision-making body of the Institute is the **Scientific Council** of 15 members elected by the employees of the Institute (Table 2). Presently Dr.phys. L.Trinklere is the elected chairperson of the ISSP Council. The Council appoints director and its deputies. New elections of the Council were held in 2016.

The Scientific Council in June 2016 elected a new director – the former deputy director for research of ISSP Dr. phys. Martins Rutkis.

The interdisciplinary research at the ISSP is performed by its highly qualified staff. At end of 2017 there were 196 employees working at the Institute, 20 of 117 members of the research staff hold Dr.habil.degrees, 65 hold Dr. or PhD. At the end of 2017 there were 16 PhD students and 48 undergraduate and graduate students in physics, chemistry, material science and optometry programmes working at the ISSP.

Table 1

ORGANIZATIONAL STUCTURE OF THE ISSP IN 2017

Table 2

The Scientific Council of the Institute, elected in 2016

1. Laima Trinklere, Dr.phys., chairperson of the Council
2. Marcis Auzins, Dr.habil.phys., UL
3. Gunars Bajars, Dr.chem.
4. Jurģis Grūbe, PhD student
5. Mārtins Rutkis, Dr.phys.
6. Andrejs Silins, Prof., Dr.habil.phys.
7. Anatolijs Sharakovskis, Dr.phys.
8. Andris Sternbergs, Dr.habil.phys.
9. Anatolijs Truhins, Dr.habil.phys.

10. Andris Anspoks, Dr.phys.
11. Dmitrijs Bočarovs, Dr.phys.
12. Jānis Kleperis, Dr.phys.
13. Māris Knite, Dr.Phys., RTU professor
14. Donāts Millers, Dr.habil.phys.
15. Aivars Vembris, Dr.phys.

The annual report summarizes the research activities of the ISSP in 2017. The table below presents the key performance indicators of ISSP:

Key performance indicators for Research	**3 years avrg.(2013-2015)**	**2016**	**2017**	**2018 (estimated)**	**2019 (Mid-CAMART²)**	**2023 (End of CAMART²)**	**2026 (Sustainability)**
Number of scientific publications according to "Scopus"	116	96	**93**	120	200	300	400
Fraction of scientific publications in Int. Collaboration (%)	51	74	**61**	62	55	60	65
Number of citations/year according to "Scopus"	1545	1908	**1657**	1800	2 000	2 500	5 000
Average SNIP per publications	0.790	0.748	**0.896**	0.920	1.000	1.100	1.250
Number of scientific and technical personnel (FTE)	105	113	**117**	120	130	170	180
Publications/FTE	1.11	0.85	**0.79**	1.00	1.54	1.76	2.22
Gender balance of scientific and technical personnel (% female)	26	24.5	**22.2**	24.0	30	33	37

The analysis of Key performance indicators (KPIs) is reported in the Action Plan for 2018.

Scientific Highlights

ISSP UL contribution into the most significant achievements of Latvian science in 2017

Novel materials for infrared light convertors and white light sources

U. Rogulis, M. Spriņģis, A. Šarakovskis, J. Grūbe, A. Fedotovs, E. Elsts, G. Krieķe, A. Antuzevičs, M. Ķemere

Institute of Solid State Physics, University of Latvia, Kengaraga Street 8, LV-1063, Riga, Latvia

Novel transparent glass ceramics with fluoride nanocrystals doped with rare-earth ions have been sintered. The important optical properties for applications have been optimized, by controlling the size of the nanocrystals and concentration of the rare-earth ions, namely, the luminescence efficiency and the colour of the emitted light. The obtained oxyfluoride glasses and glass ceramics efficiently transform the infrared radiation (IR) into the visible light (Figure 1). By variation of the chemical composition, we obtained materials which emit eye-pleasant white light, are long-term durable and applicable in the light sources (Figure 2). The efficiency of the materials and compatibility with optical waveguides allow one to use them for the development of optical sensors and IR visualisation.

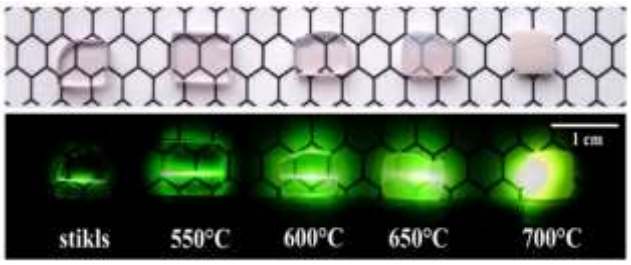

Figure 1. Luminescence of IR irradiated oxyfluoride glasses and glass-ceramics obtained at different temperatures.

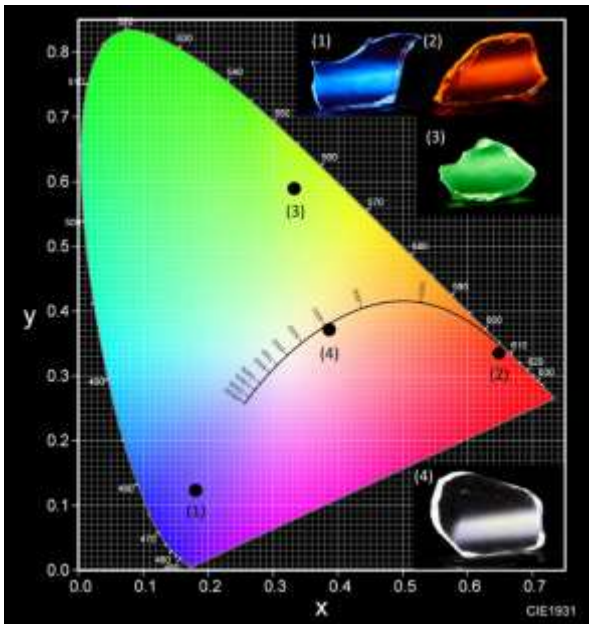

Figure 2. UV excited photoluminescence of rare-ions activated oxyfluoride glasses and glass-ceramics (1), (2), (3), (4) and corresponding colour coordinates in the CIE1931 colour diagram.

Published in:

1. G. Krieke, A. Sarakovskis, R. Ignatans, J. Gabrusenoks, Journal of the European Ceramic Society 37 (2017) 1713-1722, DOI: 10.1016/j.jeurceramsoc.2016.12.023 (IF=3.411, SNIP=1.776).

2. G. Krieke, A. Sarakovskis, M. Springis, Journal of Alloys and Compounds 694 (2017) 952-958, DOI: 10.1016/j.jallcom.2016.10.156 (IF=3.133, SNIP=1.321).

3. M. Kemere, J. Sperga, U. Rogulis, G. Krieke, J. Grube, Journal of Luminescence 181 (2017) 25-30, DOI: 10.1016/j.jlumin.2016.08.062 (IF=2.686, SNIP=1.140).

4. A. Antuzevics, M. Kemere, G. Krieke, R. Ignatans, Optical Materials 72 (2017) 749-755, DOI: 10.1016/j.optmat.2017.07.024 (IF=2.238, SNIP=1.055).

I. Functional materials for electronics and photonics.

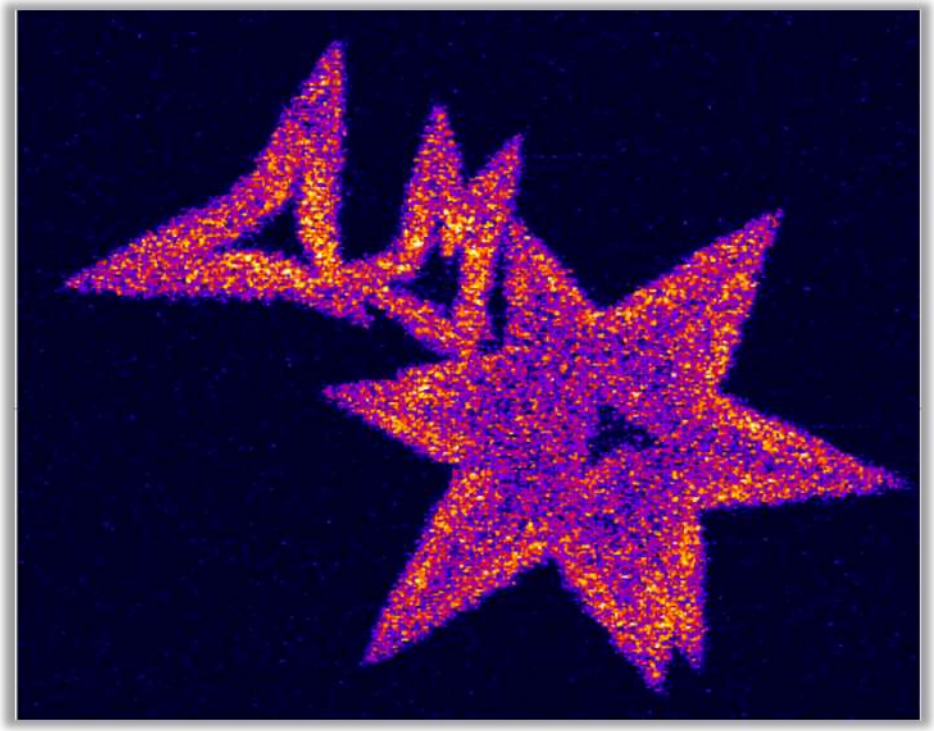

Unveiling molecular changes in water by small luminescent nanoparticles

L. Labrador-Páez[a], D.J. Jovanović[b], M.I. Marqués[c,d], K. Smits[e], S.D. Dolić[b], F. Jaque[d], H. E. Stanley[f], M.D. Dramicánin[b], J. García-Solé[a], P. Haro-González[a], D. Jaque[a]

[a] *Institute Departamento de Física de Materiales, Universidad Autónoma de Madrid, Madrid 28049, Spain*
[b] *Vinc˘a Institute of Nuclear Sciences, University of Belgrade, Belgrade 11001, Serbia*
[c] *Departamento de Física de Materiales, Universidad Autónoma de Madrid,Madrid 28049, Spain*
[d] *Condensed Matter Physics Center (IFIMAC) and Nicolás Cabrera Institute, Universidad Autónoma de Madrid, Madrid 28049, Spain*
[e] *Institute of Solid State Physics, University of Latvia, Kengaraga Street 8, LV-1063, Riga, Latvia*
[f] *Center for Polymer Studies and Department of Physics Boston University MA 02215, USA*

Nowadays a large variety of applications is based on solid nanoparticles dispersed in liquids — so called nanofluids. The interaction between the fluid and the nanoparticles plays a decisive role in the physical properties of the nanofluid. A novel approach based on the nonradiative energy transfer between two small luminescent nanocrystals ($GdVO_4:Nd^{3+}$ and $GdVO_4:Yb^{3+}$) dispersed in water is used in this work to investigate how temperature affects both the processes of interaction between nanoparticles and the effect of the fluid on the nanoparticles. From a systematic analysis of the effect of temperature on the $GdVO_4:Nd^{3+}$ → $GdVO_4:Yb^{3+}$ interparticle energy transfer, it can be concluded that a dramatic increase in the energy transfer efficiency occurs for temperatures above 45 °C. This change is properly explained by taking into account a crossover existing in diverse water properties that occurs at about this temperature.

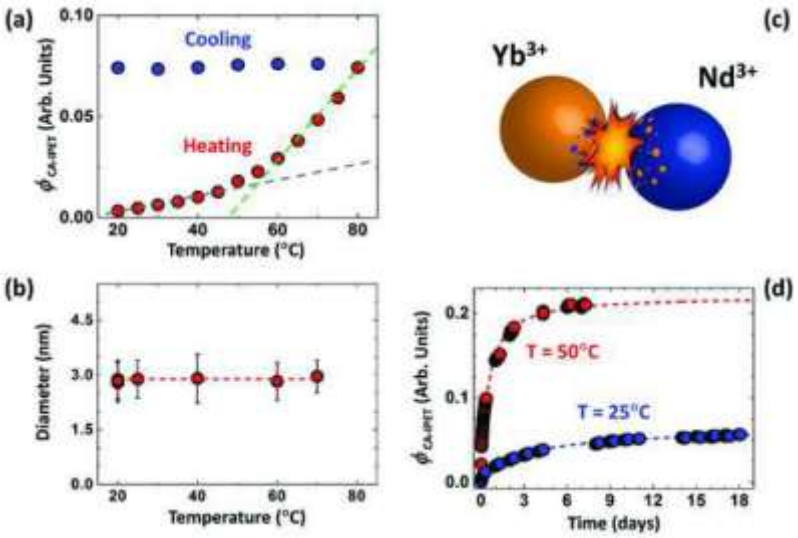

Dependence of IPET efficiency on temperature. a) Temperature dependence of the CA-IPET efficiency as obtained during a heating (black) and cooling (gray) cycle. b) Diameter of the SLNPs estimated from TEM images of mixed LNF heated at diverse temperatures. c) Schematic representation of a collision-assisted interparticle ion exchange process. d) Long-term evolution of CA-IPET efficiency as obtained at two different temperatures (25 °C (gray) and 50 °C (black)).

The obtained results allow elucidation on the molecular arrangement of water molecules below and above this crossover temperature. In addition, it is observed that an energy transfer process is produced because of interparticle collisions that induce irreversible ion exchange between the interacting nanoparticles.

Published in:
L. Labrador-Páez, D.J. Jovanović, M.I. Marqués, K. Smits, S.D. Dolić, F. Jaque, H. E. Stanley, M.D. Dramicánin, J. García-Solé, P. Haro-González, D. Jaque, Small 13 (2017) 1700968, DOI: 10.1002/smll.201700968 (IF=8.643, SNIP=1.505).

Luminescence and Raman detection of molecular Cl_2 and ClClO molecules in amorphous SiO_2 matrix

L.Skuja[a], K. Kajihara[b], K. Smits[a], A. Silins[a], H. Hosono[c]

[a] *Institute of Solid State Physics, University of Latvia, Kengaraga Street 8, LV-1063, Riga, Latvia*
[b] *Department of Applied Chemistry, Graduate School of Urban Environmental Sciences, Tokyo Metropolitan University, 1-1 Minami-Osawa, Hachioji, Tokyo 192-0397, Japan*
[c] *Laboratory for Materials and Structures & Materials Research Center for Element Strategy, Tokyo Institute of Technology, 4259 Nagatsuta, Midori-ku, Yokohama 226-8503, Japan*

Amorphous (glassy) silicon dioxide SiO_2 is one of the most important contemporary optical materials: nearly all optical fiber waveguides are manufactured from glassy SiO_2. This is due to its exceptionally high optical transparency, extending from the near-infrared spectral range (1200-1600 nm) used for optical communication fibers, through the visible range down to the vacuum-ultraviolet (V-UV) wavelengths (160 nm). Therefore, apart from the telecom fibers, many specific applications of fibers in medicine, laser processing of materials, sensors, analytical instrumentation, using visible/UV ranges have emerged.

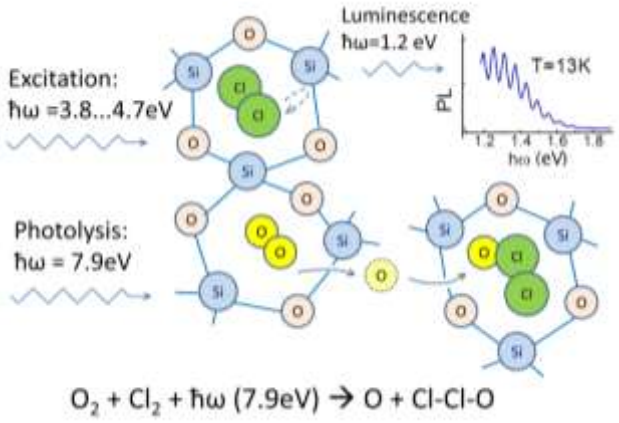

Behavior of Cl_2molecules in SiO_2 glass. On excitation by UV photons dissociation is prevented by SiO_2 "cage", retaining Cl molecule together, which goes to triplet state manifested by a characteristic Cl_2 luminescence. High energy photons dissociate interstitial O_2 molecules, and mobile O atoms enter the cage and form ClClO molecules, detected by their Raman signal.

Glassy SiO_2 is manufactured by oxidizing $SiCl_4$. This process ensures the parts-per-billion level purity necessary for telecom fibers. However, much higher amount of Cl impurities remains in glass, either in the form of interstitial Cl_2 molecules or bound Si-Cl groups and decreases the ultraviolet transparency of SiO_2.

Our work is the first report of detailed spectroscopic parameters of Cl_2 molecules in SiO_2 and their photochemical behavior. It was found that they give a very characteristic low temperature luminescence, which can be used as high-sensitivity diagnostic tool for detecting the presence of Cl_2 in SiO_2. Our data indicate that Cl_2 is stabilized in SiO_2 by the "cage effect", and Cl_2 atoms cannot easily leave the SiO_2 interstices on photodissociation.

By using high-sensitivity Raman technique, we identified the Raman signal of interstitial Cl_2 in SiO_2 (546 cm^{-1}). In UV excimer-laser irradiated glass we found a new signal at 954 cm^{-1}, which can be assigned to interstitial Cl-Cl-O, formed when interstitial O atom enters the Cl_2 cage. Optical absorption by ClClO may be detrimental to optical fibers for UV-related applications.

Published in:
L. Skuja, K. Kajihara, K. Smits, A. Silin, H. Hosono, The Journal of Physical Chemistry C 121 (2017) 5261-5266, DOI: 10.1021/acs.jpcc.6b13095 (IF=4.536, SNIP=1.181).

Doped zirconia phase and luminescence dependence on the nature of charge compensation

K. Smits[a], D. Olsteins[a], A. Zolotarjovs[a], K. Laganovska[a], D. Millers[a], R. Ignatans[a], J. Grabis[b]

[a] *Institute of Solid State Physics, University of Latvia, Kengaraga Street 8, LV-1063, Riga, Latvia*
[b] *Institute of Inorganic Chemistry, Riga Technical University, Latvia*

Zirconia is a relatively new material with many promising practical applications in medical imaging, biolabeling, sensors, and other fields. In this study we have investigated lanthanide and niobium doped zirconia by luminescence and XRD methods. It was proven that charge compensation in different zirconia phases determines the incorporation of intrinsic defects and activators. Thus, the structure of zirconia does not affect the Er luminescence directly; however, it strongly affects the defect distribution around lanthanide ions and the way in which activator ions are incorporated in the lattice.

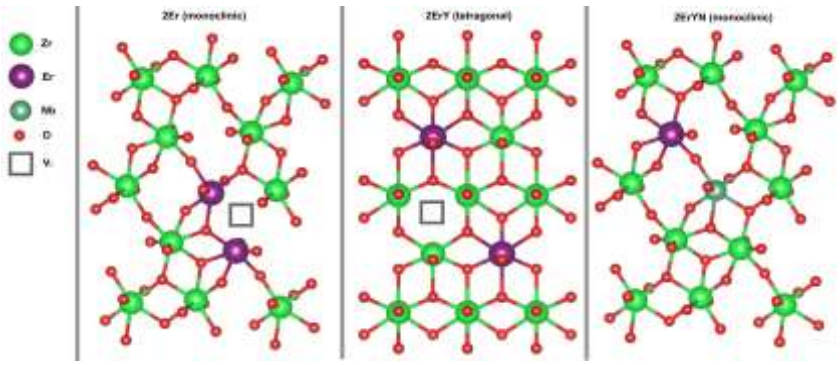

Possible mechanisms for the incorporation of Er ion and oxygen vacancies in tetragonal, monoclinic and Nb doped monoclinic zirconia.

Our results demonstrate the correlation between the crystalline phase of zirconia and charge compensation, as well as the contribution of different nanocrystal grain sizes. In addition, our experimental results verify the theoretical studies of metastable (tetragonal, cubic) phase stabilization determined using only oxygen vacancies. Moreover, it was found that adding niobium drastically increases activator luminescence intensity, which makes Ln^{3+} doped zirconia even more attractive for various practical applications.

Although this study was based on the luminescence of the Er ion, the phase stabilization, charge compensation, and luminescence properties described in our results are expected to be similar for other lanthanide elements. Our results suggest that the luminescence intensity of other oxide matrices where lanthanides incorporate in place of tetravalent cations could be increased by addition of Nb ions.

Published in:
K. Smits, D. Olsteins, A. Zolotarjovs, K. Laganovska, D. Millers, R. Ignatans, J. Grabis, Scientific Reports 7 (2017) 44453, DOI: 10.1038/srep44453 (IF=4.259, SNIP=1.401).

Phase transitions and upconversion luminescence in oxyfluoride glass ceramics containing $Ba_4Gd_3F_{17}$ nanocrystals

G. Krieke, A. Sarakovskis, R. Ignatans, J. Gabrusenoks

Institute of Solid State Physics, University of Latvia, Kengaraga Street 8, LV-1063, Riga, Latvia

Recently considerable attention has been devoted to investigation of rare earth doped materials for upconversion luminescence. Among others oxyfluoride glass ceramics containing barium rare earth fluoride nanocrystals are excellent candidates for applications in which transparency is required.

In this study novel transparent Er^{3+} doped oxyfluoride glass-ceramics containing $Ba_4Gd_3F_{17}$ nanocrystals were prepared by melt quenching followed by heat treatment of as-prepared glasses. The phase composition, microstructure were investigated by X-ray diffraction, scanning electron microscopy and transmission electron microscopy. The spectroscopic properties of glass ceramics were compared with single phase cubic and rhombohedral $Ba_4Gd_3F_{17}$ ceramics. The local environment of Er^{3+} and the phonon energy of both polymorphs were analyzed using luminescence and Raman spectroscopy.

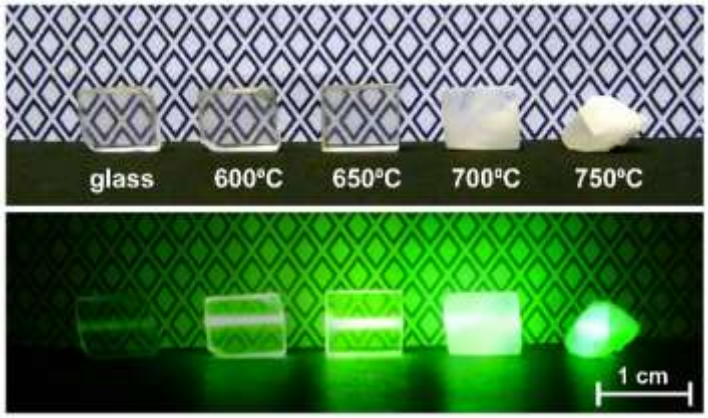

Photographs of the Er^{3+} doped glass and glass ceramics heat treated at different temperatures: upper row – as prepared, lower row – excited with 975 nm laser.

In the temperature range of 650-700°C, a phase transition from metastable cubic to rhombohedrally distorted fluorite phase in the glass ceramics was detected using Er^{3+} as a probe.

Intense upconversion luminescence resulting from energy transfer between erbium ions was observed under near-infrared excitation (975 nm). Longer characteristic decay times and splitting of the luminescence bands compared to the precursor glass indicated the incorporation of erbium ions in the crystalline phase. The intensity of the upconversion luminescence in the glass ceramics with rhombohedral $Ba_4Gd_3F_{17}$ nanocrystals was two orders of magnitude higher than in the precursor glass and at least two times higher than in the cubic phase.

In conclusion, low local symmetry of RE^{3+} (C_1) and low effective phonon energy (310 cm^{-1}) of rhombohedral $Ba_4Gd_3F_{17}$ nanocrystals make this glass ceramics a desirable host for UCL applications.

Published in:
G. Krieke, A. Sarakovskis, R. Ignatans, J. Gabrusenoks, Journal of the European Ceramic Society 37 (2017) 1713-1722, DOI: 10.1016/j.jeurceramsoc.2016.12.023 (IF=3.411, SNIP=1.776).

II. Nanotechnology, nanocomposites and ceramics.

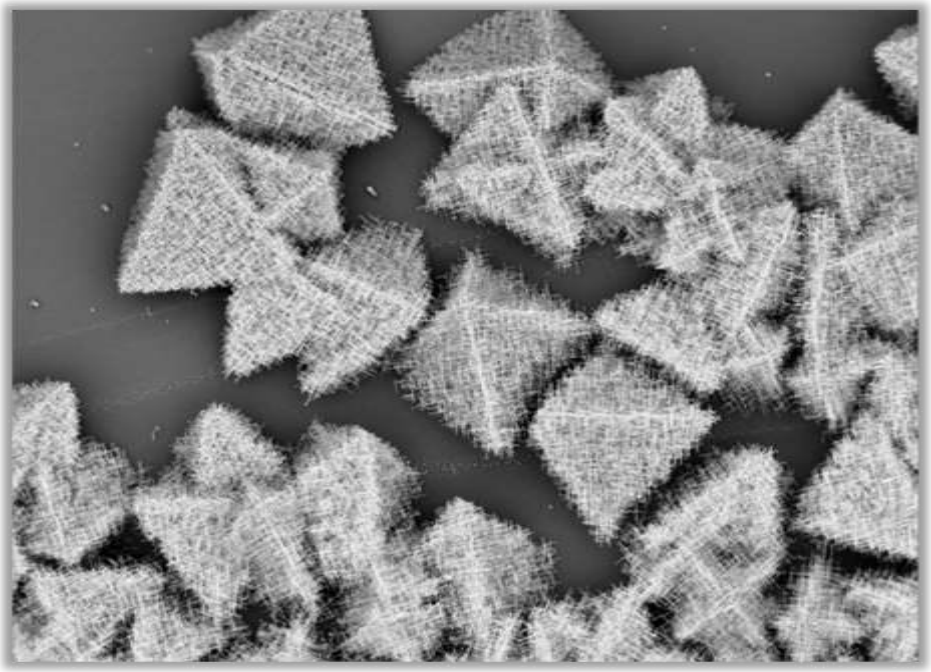

Enhanced flexibility and electron-beam-controlled shape recovery in alumina-coated Au and Ag core-shell nanowires

S. Vlassov[a], B. Polyakov[b], M. Vahtrus[a], M. Mets[a], M. Antsov[a], S. Oras[a], A. Tarre[a], T. Arroval[a], R. Lõhmus[a], J. Aarik[a]

[a] *Institute of Physics, University of Tartu, W. Ostwaldi 1, 50411, Tartu, Estonia*
[b] *Institute of Solid State Physics, University of Latvia, Kengaraga 8, LV-1063, Riga, Latvia*

The properties of nanowires (NWs) can be efficiently modified by coating them with a thin layer of another material, resulting in the formation of a 1D core-shell-type heterostructure. In the simplest case, the coating is used as a dielectric spacer for isolation purposes in nanoscale electronics, but it can be also employed to enhance certain properties of 1D nanostructures (NS) and to improve their functionalities. Oxide coatings, such as SiO_2 and Al_2O_3, can strongly enhance the optical properties of metallic NWs, as surface plasmons confine electromagnetic fields near the metal-dielectric interface, permitting the overcoming of the conventional diffraction limit of dielectric optics. Therefore, metal oxide core-shell NWs are promising candidates for dense on-chip integrated circuits for next generation information technology, solar cells, and LED devices based on single 1D NS. Such a coating is also expected to improve the mechanical characteristics of 1D NS.

Herein, we investigated the influence of e-beam irradiation on mechanical behavior of alumina-coated Ag and Au NWs under bending deformations. The NWs were coated with Al_2O_3 by the atomic layer deposition method and studied inside a high-resolution scanning electron microscope (HR-SEM) equipped with a nanomanipulator. The influence of the alumina coating on the mechanical properties was also studied in bending tests performed with an atomic force microscope (AFM) in the absence of an e-beam.

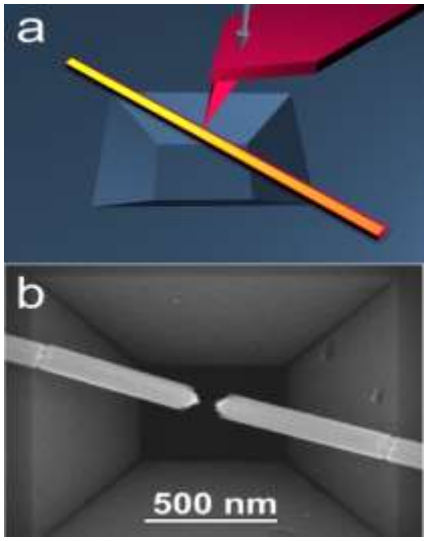

Schematics of three-point bending test (a). SEM image of alumina-coated Au NWs broken after the AFM bending test (b).

AFM tests revealed that coating protected the core material from the fracture and plastic yield, allowing it to withstand significantly higher deformations and stresses in comparison to uncoated NWs. The most important finding was that even at moderate accelerating voltage and probe current values, the e-beam was capable of inducing reversible elastic-to-plastic transition in Ag/Al_2O_3 and Au/Al_2O_3 NWs. Without e-beam irradiation, the core-shell NWs behaved elastically, while under e-beam irradiation, it was possible to freeze the bent core-shell NW at any arbitrary curvature below the yield strength of the core materials and later restore its initially straight profile by irradiating the NW with electrons. Therefore, an e-beam has great potential for controlled modulation of the mechanical properties of amorphous oxide nanomaterials and offers advanced flexibility in the assembly of NW-based systems.

Published in:
S. Vlassov, B. Polyakov, M. Vahtrus, M. Mets, M. Antsov, S. Oras, A. Tarre, T. Arrova, R. Lõhmus, J. Aarik, Nanotechnology 28 (2017) 505707 (10pp), DOI: 10.1016/j.actamat.2017.02.074 (IF=3.4, SNIP=0.8).

Upconversion luminescence of a transparent glass ceramics with hexagonal $Na(Gd,Lu)F_4$ nanocrystals

G. Krieke, A. Sarakovskis, M. Springis

Institute of Solid State Physics, University of Latvia, Kengaraga Street 8, LV-1063, Riga, Latvia

Transparent oxyfluoride glass ceramics are composites that combine the good chemical and mechanical stability of oxide glasses with the excellent optical properties of fluoride crystals. These materials are ideal hosts for rare earth ions due the low phonon energy of fluorides reduces the nonradiative relaxations therefore they suitable candidates for infrared to visible upconversion luminescence (UCL) processes. Among others, hexagonal $NaLuF_4$ is considered highly efficient host for UCL surpassing other $NaREF_4$ (RE-rare earth ion). Unfortunately, only its high temperature polymorph cubic $NaLuF_4$ has been obtained in the glass ceramics, therefore this research is devoted to the stabilization of hexagonal phase by formation of $Na(Gd,Lu)F_4$ solid solutions.

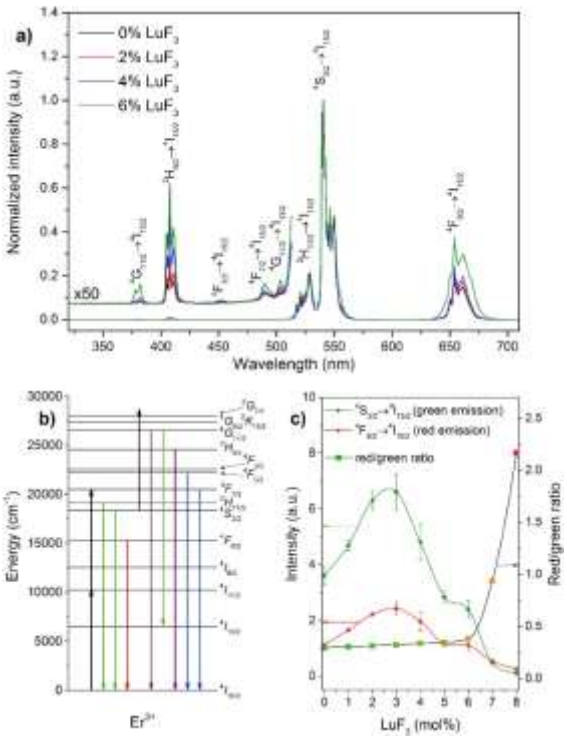

a) UCL spectra of β-$Na(Gd,Lu)F_4$ glass ceramics with 0, 2, 4 and 6 mol% LuF_3 doped with 1% ErF_3 excited with 975 nm CW laser, b) energy level scheme of Er^{3+} and c) UCL intensity and red to green luminescence intensity ratio dependence on LuF_3 content in glass.

In this study novel Er^{3+} doped transparent glass ceramics containing hexagonal $Na(Gd,Lu)F_4$ nanocrystals were prepared using melt quenching and subsequent heat treatment of precursor glasses with molar composition of $17Na_2O$-7NaF-$(8-x)GdF_3$-$xLuF_3$-$7Al_2O_3$-$61SiO_2$ (x=0-8) doped with 0.1 and 1 mol% Er^{3+}. The distribution of rare earth ions in the crystalline and glassy phase was analyzed by X-ray diffraction and erbium luminescence decay kinetics measurement. A strong deviation of rare earth ion content in fluoride nanocrystals in comparison to the base glass was observed. Preferential incorporation of Gd^{3+} over Lu^{3+} ions in the fluoride lattice leads to the stabilization of hexagonal $Na(Gd,Lu)F_4$ structure and prevents the formation of cubic fluorite type solid solutions. An efficient UCL of Er^{3+} ions was observed under infrared excitation. With the increase of LuF_3 content in nanocrystals a gradual decrease of unit cell dimensions and lifetimes Er^{3+} emitting states was detected indicating a reduction of average distance between erbium ions in the nanocrystals. The most efficient UCL was detected for Er^{3+} doped hexagonal $Na(Gd,Lu)F_4$ glass ceramics with approximately 6 mol% LuF_3 incorporated in the hexagonal lattice, however, the maximum Lu^{3+} ions concentration reaching 45 mol% could be obtained.

Published in:
G. Krieke, A. Sarakovskis, M. Springis, Journal of Alloys and Compounds 694 (2017) 952-958, DOI: 10.1016/j.jallcom.2016.10.156 (IF=3.133, SNIP=1.321).

Thermal properties of multiferroic $Bi_{1-x}Eu_xFeO_3$ (x = 0-0.40) ceramics

S.N. Kallaev[a,b], Z.M. Omarov[a], A.G. Bakmaev[a], R.G. Mitarov[c], L.A. Reznichenko[d], K. Bormanis[e]

[a] *Institute of Physics, Dagestan Science Centre, RAS, 367003, Makhachkala, Russia*
[b] *Dagestan State University, 367045, Makhachkala, Russia*
[c] *Dagestan State Technical University, 367015, Makhachkala, Russia*
[d] *Southern Federal University, 344090, Rostov on Don, Russia*
[e] *Institute of Solid State Physics, University of Latvia, LV-1063, Riga Latvia*

A study of thermal diffusion, heat capacity and thermal conductivity of multiferroic $Bi_{1-x}Eu_xFeO_3$ (x=0-0.40) within the range of 130-1200 K is reported. Modifying by admixture of Eu is found to change substantially the thermal anomalies of diffusion and thermal conductivity of the antiferromagnetic phase transition, to increase heat capacity over a wide range of temperatures and to shift the antiferromagnetic transition temperature. The excess heat capacity is shown being related to Schottky effect of three-level states. The mechanisms dominating thermal transfer of phonons at the phase transition and dependence of the mean free path of phonons on the temperature are determined.

The studied ceramic solid solution samples of $Bi_{1-x}Eu_xFeO_3$ obtained from high-purity oxides by conventional solid phase 2-stage synthesis with intermediate grinding and granulation of the powder and consecutive baking under atmospheric conditions were chosen to be within the x=0-0.40 range of Eu admixture concentrations.

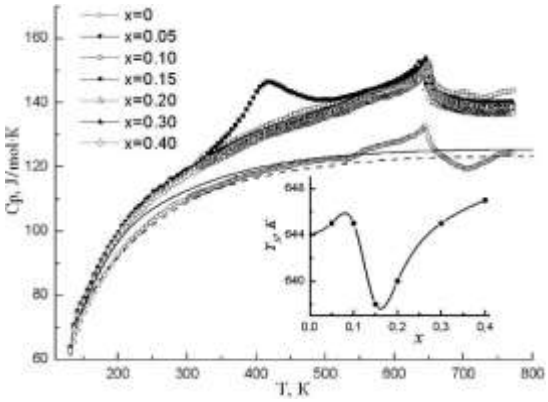

Heat capacity of $Bi_{1-x}Eu_xFeO_3$ (x = 0-0.40) as a function of temperature. Dotted and solid lines - approximations of phonon heat capacity of $BiFeO_3$ and $Bi_{1-x}Eu_xFeO_3$ with Debye function, respectively. Insert - Neel temperature T_N as a function of concentration.

Specific heat capacity C_p of the $Bi_{1-x}Eu_xFeO_3$ (x = 0, 0.05, 0.10, 0.15, 0.20, 0.30, 0.40) multiferroics shows an anomaly at the antiferromagnetic phase transition temperature T_N. Noticeable anomalies are seen on the thermal diffusion $\eta(T)$ and thermal conductivity $\lambda(T)$ curves around the temperature of the antiferromagnetic phase transition $T_N \approx 643$ K. A significant shift of the temperature of antiferromagnetic phase transition and an additional contribution to heat capacity within the 140-800 K range is caused by Eu admixture, which can be interpreted as Schottky anomaly of triple states.

Results of the present study together with available structural and acoustic data suggest that local distortions of the lattice raised by deformations of the FeO_6 octahedra and polar shifts of Bi^{3+} and Fe^{3+} ions pose the main centres of phonon scattering. Admixture of Eu is found to cause considerable change of the anomalies of thermal diffusion and thermal conductivity at phase transitions - appearance of minimum at the antiferromagnetic transition around T_N and broadening of the ferroelectric transition at T_C.

Published in:
S.N. Kallaev, Z.M. Omarov, A.G. Bakmaev, R.G. Mitarov, L.A. Reznichenko, K. Bormanis, Journal of Alloys and Compounds 695 (2017) 3044-3047, DOI: 10.1016/j.jallcom.2016.11.347 (IF=3.133, SNIP=1.321).

Radioluminescence, thermoluminescence and dosimetric properties of ZnO ceramics

L. Grigorjeva[a], A. Zolotarjovs[a], S. Yu. Sokovnin[b,c], D. Millers[a], K. Smits[a], V. G. Il`ves[b,c]

[a] *Institute of Solid State Physics, University of Latvia, Kengaraga 8, LV-1063, Riga, Latvia*
[b] *Institute of Electrophysics, Ural Branch, Russian Academy of Sciences, 106 Amundsen Street, Yekaterinburg 620016, Russia*
[c] *Ural Federal University, 19 Mira Street, Yekaterinburg 620016, Russia*

In recent years the ZnO attracted many researchers due to its possible applications as transparent conductive electrodes, particle detectors, fast scintillators, sensors and others. The peak position of defect luminescence band needed for most of these practical applications, its intensity and decay kinetics are very sensitive to the type and morphology of ZnO as well as to the synthesis method used, annealing conditions, doping and other parameters. Unfortunately, up to now the defect pairs responsible for the luminescence are not completely identified. Therefore, the following study was performed to get closer to the understanding of the processes.

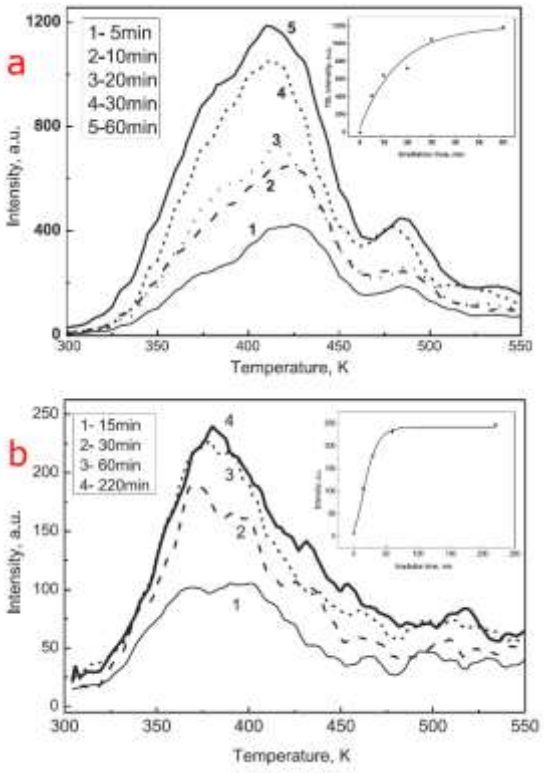

TSL and TSL intensity dependence on irradiation time (inset) for ceramic 1 (a) and ceramic 2 (b).

Two types of ZnO ceramics were fabricated and characterized by XRD, SEM methods. The radioluminescence spectra were measured within the 300-550 K range. The defect luminescence band peaking at about 2.35 eV is the dominant one in radioluminescence spectra in both of the fabricated ceramics. The thermostimulated luminescence (TSL) glow-curves were measured after X-ray irradiation at 300 K. It was concluded that the complex overlapping peak within the 320-450 K temperature range consists of two components (about 360-375 K and 400-420 K). The ratio of component intensities differs in both ceramics. The positions of high temperature TSL components (480-520 K) also differ in both samples; therefore not only sintering conditions but also the properties of the initial powder are very important for characteristics of TSL. A linear dependence of peak intensity on irradiation dose was observed up to about 3 kGy for ceramic 1 and up to 9 kGy for ceramic 2.

Published in:
L. Grigorjeva, A. Zolotarjovs, S. Sokovnin, D. Millers, K. Smits, V. Il'ves, Ceramics International 43 (2017) 6187-6191, doi:10.1016/j.ceramint.2017.02.016 (IF=2.986, SNIP=1.304).

III. Thin films and coating technologies.

Thin film organic thermoelectric generator based on tetrathiotetracene

K. Pudzs[a], A. Vembris[a], M. Rutkis[a], S. Woodward[b]

[a] *Institute of Solid State Physics, University of Latvia, Kengaraga Street 8, LV-1063, Riga, Latvia*
[b] *GSK Carbon Neutral Laboratory for Sustainable Chemistry, University of Nottingham, Jubilee Campus, Nottingham NG7 2GG, UK*

Thin films of p- and n-type organic semiconductors for thermoelectrical (TE) applications are produced by doping of tetrathiotetracene (TTT). To obtain p-type material TTT is doped with iodine during vacuum deposition of thin films or by postdeposition doping using controlled exposure to iodine vapors. Thermal co-deposition in vacuum of TTT and tetracyanoquinodimethane (TCNQ) is used to prepare n-type thin films. The attained thin films are characterized by measurements of the Seebeck coefficient and electrical conductivity. The Seebeck coefficient and conductivity can be varied by altering the doping level.

We have demonstrated that by appropriate doping of (potentially) low cost TTT it is possible to obtain TE active organic thin films of both p- and n-types. We have prepared p-type TTT iodide thin films with a power factor of 0.52 μW m^{-1} K^{-2}, an electrical conductivity of 130 S m^{-1}, and a Seebeck coefficient of 63 μV K^{-1} and n-type TCNQ:TTT films with a power factor of 0.33 μW m^{-1} K^{-2}, an electrical conductivity of 57 S m^{-1}, and a Seebeck coefficient of −75 μV K^{-1}.

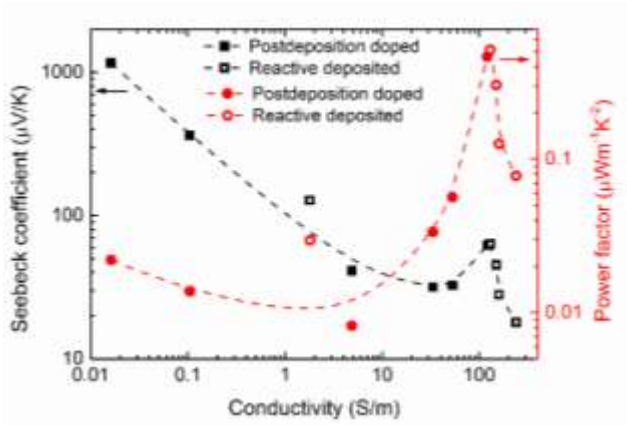

Dependence of the Seebeck coefficient and power factor on electrical conductivity of TTT iodide doped thin films for reactive deposited (hollow symbols) and postdeposition doped samples (filled symbols).

This achievement has allowed demonstration of the feasibility of thin film TEG based on organic p- and n-type materials operating under near ambient conditions. Single couple thin film TEGs were made by deposition of both p- and n-type TTT based materials on one substrate in two separated deposition cycles. Particularly a “proof of concept” single couple TEG of p-type TTT iodide thin films coupled with n-type thin films produced by co-deposition of TTT and TCNQ were prepared. The simple fabrication process proposed allows easy duplication of such TEG modules therefore the power of device could be multiplied several times. Power of 5.5 pW K^{-1} was measured for fabricated single couple TEG close to room temperature. This value is mainly limited due to electrical conductivity of polycrystalline thin films. Two options to improve conductivity are proposed: one is optimizing crystallite orientation in thin film plane, another is to reduce the impact of grain boundaries on charge carrier mobility by developing denser packing of polycrystalline thin films. Opportunities to increase thin film electrical conductivity should be pursued to raise the power output of the thin films.

Published in:
K. Pudzs, A. Vembris, M. Rutkis, S. Woodward, Advanced Electronic Materials 3 (2017) 1600429, DOI: 10.1002/aelm.201600429 (IF=4.193, SNIP=0.567).

Donor and acceptor substituted triphenylamines exhibiting bipolar charge-transporting and NLO properties

D. Gudeika[a], A. Bundulis[b], I. Mihailovs[b], D. Volyniuk[a], M. Rutkis[b], J.V. Grazulevicius[a]

[a] *Department of Polymer Chemistry and Technology, Kaunas University of Technology, Radvilenu pl. 19, LT-50254, Kaunas, Lithuania*

[b] *Institute of Solid State Physics, University of Latvia, Kengaraga Street 8, LV-1063, Riga, Latvia*

Low-molar-mass amorphous molecular materials having intramolecular charge transfer properties represent an interesting class of materials which attracts increasing attention. Compared to polymeric compounds, where batch to batch synthetic reproducibility, purification and product characterization are often rather difficult tasks, the molecular materials are much easier to obtain, isolate, identify and purify. Organic materials having triphenylamino moiety have attracted attention of both experimental and theoretical communities due to their useful thermal, electrochemical, photoelectrical and photophysical properties. The electron-donating nature of triphenylamino moiety predetermines good hole-transporting properties and low ionization potentials of the layers of the triphenylamine derivatives.

In this paper, we synthesized donor-acceptor type triphenylamine-based malonodinitriles and studied their thermal, optical, photophysical, electrochemical and nonlinear optical properties. The derivatives of triphenylamine containing the different numbers of electron-accepting dicyanovinyl and electron-donating methoxy or methyl groups were obtained by the Knoevenagel condensation reaction. The synthesized compounds form molecular glasses with glass transition temperatures ranging from 38 to 107 ^{0}C. The hole mobility values of methoxy-substituted compounds were in the range of 10^{-7} - 10^{-6} cm^2/V·s while electron mobility values reached $4.56 \cdot 10^{-4}$ cm^2/V·s at electric field of $7.5 \cdot 10^5$ V/cm. Nonlinear optical studies showed that the molecules had positive sign for second order hyperpolarizability. The smaller angle between the central plane of triphenylamino group and dicyanovinyl substituents resulted in larger second order hyperpolarizability. Also, the second order hyperpolarizability was larger for the compounds having methoxy groups as compared with those containing methyl substituents.

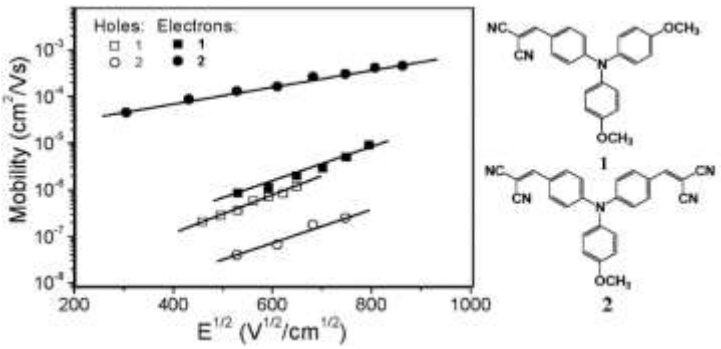

Electric field dependences of hole and electron mobilities of the layers of studied compounds 1 and 2 recorded at room temperature.

Published in:
D. Gudeika, A. Bundulis, I. Mihailovs, D. Volyniuk, M. Rutkis, J.V. Grazulevicius, Dyes and Pigments 140 (2017) 431-440, DOI: 10.1016/j.dyepig.2017.01.045 (IF=3.473, SNIP=1.039).

Stimulated emission and optical properties of pyranyliden fragment containing compounds in PVK matrix

A. Vembris[a], E. Zarins[b], V. Kokars[b]

[a] *Institute of Solid State Physics, University of Latvia, Kengaraga Street 8, LV-1063, Riga, Latvia*
[b] *Institute of Applied Chemistry, Riga Technical University, Paul Walden Street 3/7, LV-1048, Riga, Latvia*

Organic solid state lasers are thoughtfully investigated due to their potential applications in communication, sensors, biomedicine, etc. Low amplified spontaneous emission (ASE) excitation threshold value is essential for further use of the material in devices. Intramolecular interaction limits high molecule density load in the matrix. It is the case of the well-known red light emitting laser dye - 4-(dicyanomethylene)-2-methyl-6-(4-dimethylaminostyryl)-4H-pyran (DCM). The lowest ASE threshold value of the mentioned laser dye could be obtained within the concentration range between 2 and 4 wt%. At higher concentration threshold energy drastically increases. In this work optical and ASE properties of three original DCM derivatives in poly(N-vinylcarbazole) (PVK) at various concentrations will be discussed. One of the derivatives is modified DCM dye in which the methyl substituents in the electron donor part have been replaced with bulky trityloxyethyl groups (DWK-1). These sterically significant functional groups do not influence electron transitions in the dye but prevent aggregation of the molecules.

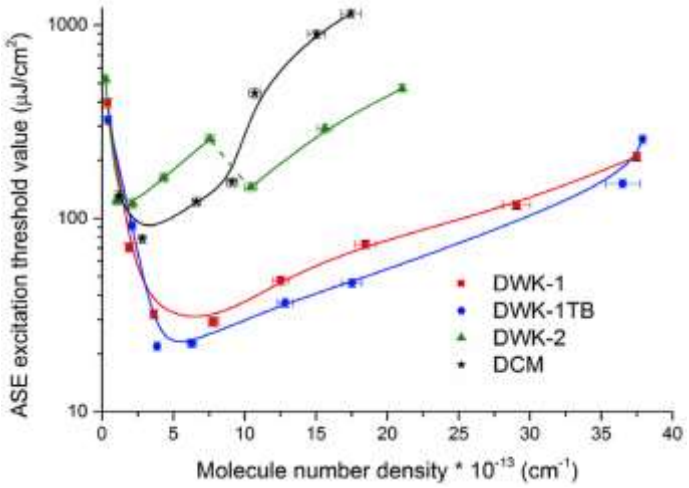

Amplified spontaneous emission excitation threshold energy for different dye load in PVK matrix.

The chemical structure of the second investigated compound is similar to DWK-1 where the methyl group is replaced with the tert-butyl substituent (DWK-1TB). The third derivative (DWK-2) consists of two N,N-di(trityloxyethyl) amino electron donor groups. All results were compared with DCM:PVK system. Photoluminescence quantum yield (PLQY) is up to ten times larger for DWK-1TB with respect to DCM systems. Bulky trityloxyethyl groups prevent aggregation of the molecules thus decreasing interaction between dyes and amount of non-radiative decays. The red shift of the photoluminescence and amplified spontaneous emission at higher concentrations were observed due to the solid state solvation effect. The increase of the investigated dye density in the matrix with a smaller reduction in PLQY resulted in low ASE threshold energy. The lowest threshold value was obtained around 21 μJ/cm^2 (2.1 kW/cm^2) in DWK-1TB:PVK films.

Published in:
A. Vembris, E. Zarins, V. Kokars, Optics and Laser Technology 95 (2017) 74-80,
DOI: 10.1016/j.optlastec.2017.04.021 (IF=2.109, SNIP=1.298).

Changes in structure and conduction type upon addition of Ir to ZnO thin films

M. Zubkins[a], R. Kalendarev[a], J. Gabrusenoks[a], A. Plaude[a], A. Zitolo[b], A. Anspoks[a], K. Pudzs[a], K. Vilnis[a], A. Azens[a], J. Purans[a]

[a] *Institute of Solid State Physics, University of Latvia, Kengaraga Street 8, LV-1063, Riga, Latvia*
[b] *Synchrotron SOLEIL, L'Orme des Merisiers, Saint-Aubin - BP 48, 91192 GIF-sur-YVETTE CEDEX, France*

Zn-Ir-O (Zn/Ir ≈ 1/1) thin films are a potential *p*-type transparent conducting oxide material. It is, however, unknown whether it is possible to achieve *p*-type conductivity at low Ir content, and how the type and the magnitude of conductivity are affected by the film structure. To investigate the changes in properties taking place at low and moderate Ir content, this study focused on the structure, electrical and optical properties of ZnO:Ir films with iridium concentration in the range of 0.0-16.4 at%. The films were deposited on glass, Si and Ti substrates by DC reactive magnetron co-sputtering at room temperature.

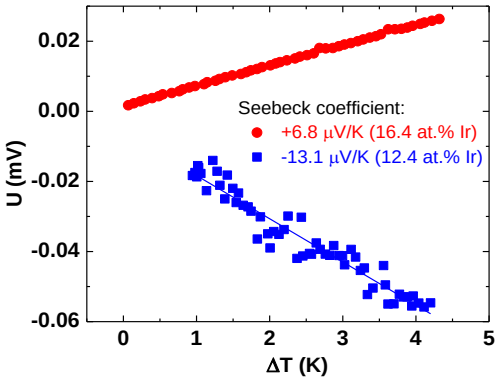

Change of the Seebeck coefficient sign from negative to positive when Ir concentration changes from 12.4 to 16.4 at. %.

ZnO:Ir thin films with Ir concentrations in the range from 0.0 to 5.1 at% contain both nano-crystallites of wurtzite w-ZnO structure and an X-ray amorphous phase. The size of the crystallites is below 10 nm, and the lattice parameters *a* and *c* are larger than those of pure ZnO crystal. The structure undergoes a transition from a wurtzite type structure to a structural atomic network different from crystalline w-ZnO in the Ir concentration range from 5.1 to 12.4 at%, according to the Fourier transform infrared spectroscopy. The structure becomes completely amorphous at the Ir concentration between 7.0 and 16.0 at%, according to the X-ray absorption spectra.

An intense Raman band at approximately 720 cm^{-1} appears upon Ir incorporation and can be ascribed to peroxide O_2^{2-} ions. ZnO:Ir thin films with an iridium concentration in the range from 0.0 to 9.5 at% are insulators. A measurable resistivity of 83 Ωcm at 12.4 at% of the iridium appears when the w-ZnO structure disappears completely. The resistivity decreases even further at 16.4 Ir at%: 2.1 Ωcm. The electrical transport changes from thermally activated hopping to metallic-like conductivity, and the conduction type undergoes a transition from n-type to p-type at an Ir concentration between 12.4 and 16.4 at%.

Absorption in the visible light band increases linearly with the iridium atomic concentration. The optical band gap of the films does not shift with the iridium concentration. However, the sharpness of the absorption edge decreases.

Published in:
M. Zubkins, R. Kalendarev, J. Gabrusenoks, A. Plaude, A. Zitolo, A. Anspoks, K. Pudzs, K. Vilnis, A. Azens, J. Purans, Thin Solid Films 636 (2017) 694-701, DOI: 10.1016/j.tsf.2017.05.049 (IF=1.879, SNIP=0.897).

IV. Theoretical and experimental studies of materials structure and properties.

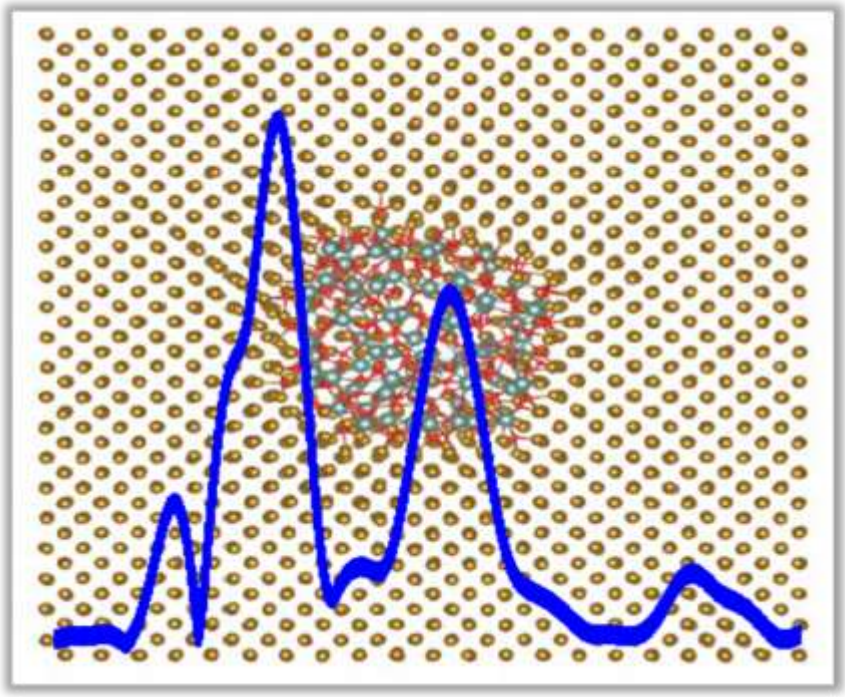

Thermal disorder and correlation effects in anti-perovskite-type copper nitride

J. Timoshenko[a,b], A. Anspoks[b], A. Kalinko[c], A. Kuzmin[b]

[a] *Department of Materials Science and Chemical Engineering, Stony Brook University, NY, 11794, USA*
[b] *Institute of Solid State Physics, University of Latvia, Kengaraga Street 8, LV-1063, Riga, Latvia*
[c] *Universität Paderborn, Naturwissenschaftliche Fakultät, Department Chemie, Warburger Straße 100, 33098, Paderborn, Germany*

So-called anti-perovskite materials have similar to perovskites crystal structure, which is described by the same formula ABX_3, but now the X site is occupied by a metal cation, while B site is occupied by light anion. The local structure and dynamics play as important role for the understanding of properties of anti-perovskites as they do in the case of perovskites.

In this study we have demonstrated on the example of antiperovskite-type Cu_3N that EXAFS analysis, coupled with reverse Monte Carlo simulations, is a powerful tool to study not only the local structure of a material, but also to probe its dynamics and correlations in atomic motion. The atomic structure of Cu_3N has been simulated using a supercell constructed based on x-ray single-crystal diffraction data, whereas the displacements of Cu and N atoms due to thermal disorder were optimized using the RMC/EA fitting procedure of the Cu K-edge EXAFS spectra.

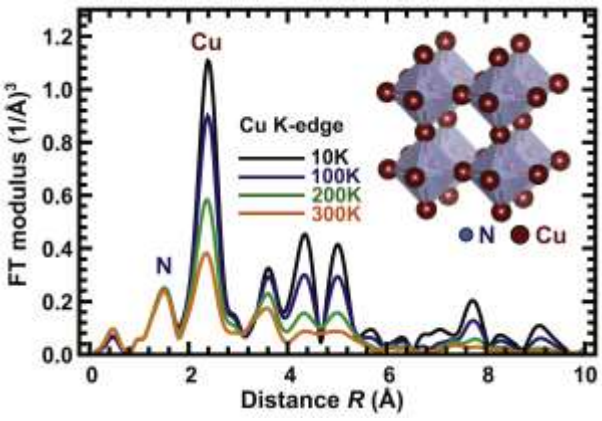

The Fourier transforms of the experimental Cu K-edge EXAFS spectra of Cu_3N at four selected temperatures.

We have found that the lattice dynamics and interatomic interactions in Cu_3N bear many resemblances with those in related perovskite-type ReO_3. Pronounced anisotropy of Cu atoms vibrations was detected in Cu_3N, as it is known for O atoms in ReO_3. Moreover, we have found that strong correlations in the motion of atoms along –N-Cu-N- atomic chains are present in Cu_3N, as was found in –Re-O-Re- atomic chains in ReO_3. Interatomic interactions in Cu_3N have also strong directional dependence, as expected for materials with pronounced covalent bonding. However, the correlations in atomic motion in Cu_3N reduces rapidly with the increase of interatomic distance, resulting in less rigid –N-Cu-N- chains. Upon temperature increase the strong anharmonic motion of Cu atoms in the direction perpendicular to Cu-N bond distorts the linear –N-Cu-N- chain, and, as a result, the average value of N-Cu-N angle decreases rapidly, in spite of Cu_3N structure remaining always cubic.

A substantial difference, nevertheless, exists between Cu_3N and both ReO_3 and metallic copper. Most importantly, the pronounced anticorrelated motion of neighboring Cu atoms occurs along Cu-Cu bonds in Cu_3N and is consistent with the breathing-type motion of NCu_6 octahedra. Such behaviour is not observed neither for O atoms in ReO_3, nor for Cu atoms in metallic copper.

Published in:
J. Timoshenko, A. Anspoks, A. Kalinko, A. Kuzmin, Acta Materialia 129 (2017) 61-71,
DOI: 10.1016/j.actamat.2017.02.074 (IF=5.301, SNIP=2.674).

Novel carbon nanotubes rolled from 6,6,12-graphyne: Double Dirac points in 1D material

D.-C. Yang[a], R. Jia[a], Y. Wang[a], C.-P. Kong[a], J. Wang[a], Y. Ma[b], R.I. Eglitis[c], H.-X. Zhang[a]

[a] *Laboratory of Theoretical and Computational Chemistry, Institute of Theoretical Chemistry, Jilin University, 130023, Changchun, China*

[b] *School of Chemistry and Chemical Engineering, Shandong University, 250100, Jinan, China*

[c] *Institute of Solid State Physics, University of Latvia, Kengaraga Street 8, LV-1063, Riga, Latvia*

The mechanical and electronic properties of 6,6,12-GNTs with varied *N* from 3 to 20 were investigated by using the density functional theory. Unlike the single-wall carbon nanotubes, the Young's moduli of 6,6,12-GNTs do not remain constant in the case of (*N*, 0), but the (0, *N*) tubes possess almost the same one around 0.32 TPa. The band structures and density of states are also exhibited in this work.

Using the DFT simulation technique we have predicted two novel carbon nanotubes, namely, (*N*, 0) and (0, *N*) 6,6,12-GNTs rolled up from the monolayer 6,6,12-graphyne, with some splendid properties. To verify the possibility of their existence, the cohesive energies as well as strain energies of the tubes have been studied. It turns out that the binding energy between the dangling bonds overcomes the strain energy from the curvature, which leads to the negative cohesive energies of the 6,6,12-GNTs. The (0, *N*) 6,6,12-GNTs have a constant Young's modulus by ~0.32 TPa, while the Young's moduli of the (*N*, 0) tubes fall on an exponential curve and can be extrapolated to 0.42 TPa. The calculated energy band maps show that the (0, *N*) 6,6,12-GNTs are semiconductors with narrow band gaps. On the contrary, the (*N*, 0) tubes are all metallic because they present an extra Dirac point in the Fermi level. The Dirac points appear in their band maps and obey an even-odd relation. The Fermi velocities and effective masses of the charge carriers have been estimated and discussed. The nonequivalent Dirac points and the difference on the direction dependence of the Fermi velocities at these Dirac points could lead the 6,6,12-GNTs to be versatile.

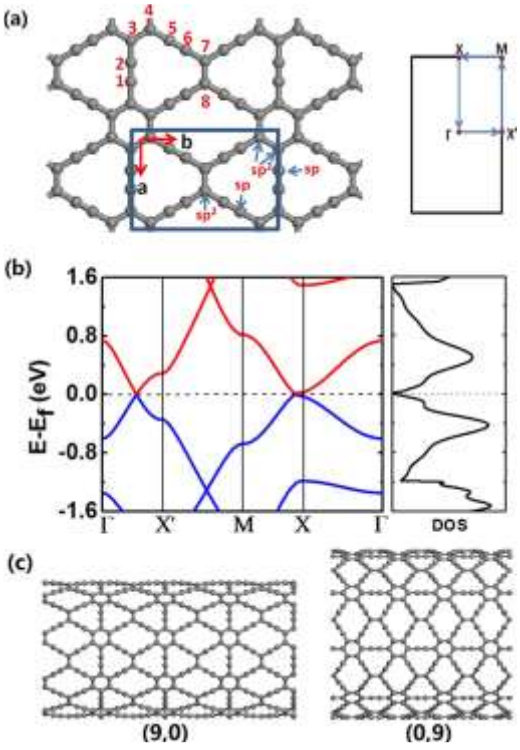

(a) Sketches for the 6,6,12-graphyne and its first Brillouin zone. (b) Band structure and DOS maps for pristine 6,6,12-graphyne. (c) Sketches for (*N*, 0) and (0, *N*) 6,6,12-GNTs; here, for example, *N*=9.

Published in:

D.-C. Yang, R. Jia, Y. Wang, C.-P. Kong, J. Wang, Y. Ma, R.I. Eglitis, H.-X. Zhang, The Journal of Physical Chemistry C 121 (2017) 14835-14844, DOI: 10.1021/acs.jpcc.7b01687 (IF=4.536; SNIP=1.181).

First-principles calculations on Fe-Pt nanoclusters of various morphologies

A. Platonenko[a], S. Piskunov[a], D. Bocharov[a], Yu. F. Zhukovskii[a], R. A. Evarestov[b], S. Bellucci[c]

[a] *Institute of Solid State Physics, University of Latvia, Kengaraga Street 8, LV-1063, Riga, Latvia*
[b] *St. Petersburg StateUniversity, 7/9 Universitetskaya nab., 199034, St. Petersburg, Russia*
[c] *INFN-Laboratori Nazionali di Frascati, Via Enrico Fermi 40, I-00044, Frascati, Italy*

Magnetic nanoparticles (NPs) with sizes ranging from 2 to 20 nm represent an important class of artificial nanostructured materials. Their magnetic properties essentially depend on the NP size because the thermal energy kT becomes comparable to the KV product term, where k T, K and V are the Boltzmann constant, the temperature, the constant of the so-called magnetic anisotropy of the NP and its volume, respectively. As a result, the magnetization of the nanocluster can randomly flip direction depending on the temperature, and thus NP can be fixed in the so-called superparamagnetic state. It was shown recently that the atomic ratio of Fe and Pt in Fe_xPt_{1-x} NPs synthesized by the sol-gel method plays an essential role for the structural and magnetic properties of these NPs. FePt NPs possessing a near-stoichiometric atomic percentage of Fe and Pt belong to the important class of magnetic nanomaterials. FePt $L1_0$ NPs have attracted considerable attention because of their extremely high magnetic anisotropy making them especially useful for practical applications in solid-state devices, e.g., in high-density magnetic recording media and in biomedicine, e.g., as contrast agents for the magnetic resonance imaging or as the basis for neutron activated coating when annealing the FePt core-shell NPs for cancer treatment.

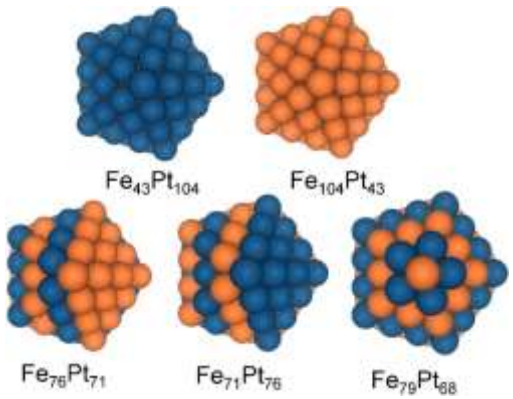

Selected icosahedral cluster models with initial morphology.

In order to shed more light on the NP surface structure and the mechanism of NP growth, we have performed large-scale DFT calculations of FePt nanoparticles of different shapes. Our calculations show that the average magnetic moment of Fe and Pt atoms does not change significantly when comparing it for bulk FePt structure and $Fe_{43}Pt_{104}$ cluster (e.g., $M_{Fe,av}$ = 3.17 μ_B and $M_{Pt,av}$ = 0.21 μ_B for $Fe_{43}Pt_{104}$ particle vs. $M_{Fe,av}$ = 3.14 μ_B and $M_{Pt,av}$ = 0.17 μ_B for FePt bulk phase). Using thermodynamical approach, we have found that the global minimum of surface energy corresponds to nanocluster with icosahedron "onion-like" structure and $Fe_{43}Pt_{104}$ morphology where the outer layer consists of Pt atoms only, which is in a good agreement with results obtained experimentally. This nanoparticle can be used for further simulations of enlarged cluster and adsorption of regular network of C atoms upon it resulting in a growth of carbon nanotubes.

Published in:
A. Platonenko, S. Piskunov, D. Bocharov, Yu.F. Zhukovskii, R.A. Evarestov, S. Bellucci, Scientific Reports, 7 (2017) 10579, DOI: 10.1038/s41598-017-11236-7 (IF=4.259, SNIP=1.401).

Use of site symmetry in supercell models of defective crystals: case of oxygen vacancy in CeO_2 and interstitials in α-Al_2O_3

R. A. Evarestov[a], D. Gryaznov[b], A. Platonenko[b], A. Chesnokov[b], Yu. F. Zhukovskii[b], E. A. Kotomin[b]

[a] *Institute of Chemistry, St. Petersburg State University, Universitetskii prospekt, 198504, St. Petersburg, Petergof, Russia*

[b] *Institute of Solid State Physics, University of Latvia, Kengaraga Street 8, LV-1063, Riga, Latvia*

It was not discussed so far that the commonly used supercell model for defective crystals imposes certain site symmetry restrictions on atoms therein. In the present study we suggest a novel approach: while choosing the supercell size of defective crystals, instead of trial-and-error approach for the defect position, it is necessary to analyze the site symmetry of the split Wyckoff positions of the perfect crystal atoms (which will be substituted and removed in the defective crystals). Then, one needs to perform defect calculations for different possible site symmetries in order to find the most energetically favorable ones. This approach could be applied to a wide class of defects in crystalline solids making the density functional calculations more effective and reliable.

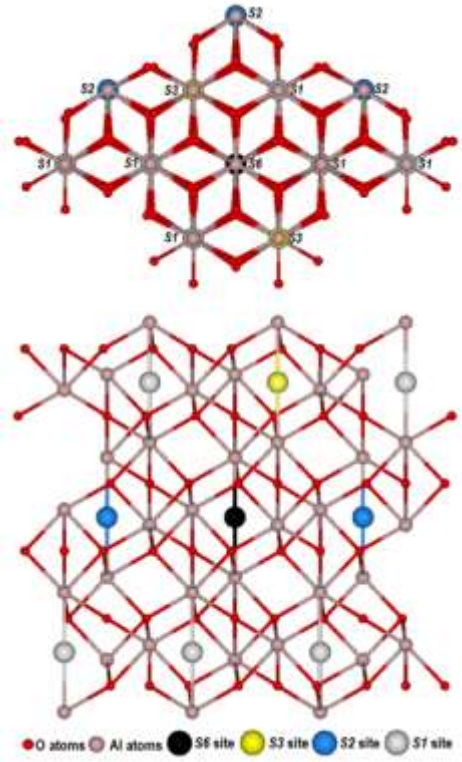

Atop (top) and aside (bottom) view of α-Al_2O_3 conventional supercell consisting of 121 atoms. The distributions of interstitial positions over 4 orbits: S6(C_{3i}), S3(C_3), S2(C_i), S1(C_1).

We have used the site symmetry approach for the hybrid density functional calculations of oxygen vacancy in CeO_2 and oxygen interstitial in α-Al_2O_3. Four positions were identified in both the cases leading to a numerous defect configurations depending on magnetic properties and/or degree of electron localization.

As a result, we were able to demonstrate that oxygen interstitial transport in α-Al_2O_3 is controlled by dumbbell bond breaking and re-forming, which is important for the prediction of radiation properties of material. Two oxygen atoms in the diamagnetic dumbbell configuration have the distance 1.44 Å typical for peroxides O_2^{2-} but the vibrational frequency of 1067 cm^{-1} and charge -1 *e* close to a free superoxide O^{2-}. Formation of small polaron configuration in the presence of oxygen vacancy in CeO_2 is possible for low symmetry configurations, namely, S2(C_s) or S4(C_{2v}), where SP denotes the site symmetry group with P point operations.

Published in:

1. R.A. Evarestov, D. Gryaznov, M. Arrigoni, E.A. Kotomin, A. Chesnokov, J. Maier, Physical Chemistry Chemical Physics 19 (2017) 8340-8348, DOI: 10.1039/c6cp08582b (IF=4.123, SNIP=1.117).

2. R.A. Evarestov, A. Platonenko, D. Gryaznov, Yu. F. Zhukovskii, E.A. Kotomin, Physical Chemistry Chemical Physics 19 (2017) 25245-25251, DOI: 10.1039/c7cp04045h (IF=4.123, SNIP=1.117).

Publications
in
Web of Science and Scopus Databases

1 **Sokolov, M., Eglitis, R.I., Piskunov, S., Zhukovskii, Y.F.**
Ab initio hybrid DFT calculations of $BaTiO_3$bulk and BaO-terminated (001) surface F-centers
International Journal of Modern Physics B, 31 (31), art. no. 1750251 .

2 **Polyakov, B., Kuzmin, A., Vlassov, S., Butanovs, E., Zideluns, J., Butikova, J., Kalendarev, R., Zubkins, M.**
A comparative study of heterostructured CuO/$CuWO_4$ nanowires and thin films
Journal of Crystal Growth, 480, pp. 78-84.

3 **Rusevich, L.L., Zvejnieks, G., Erba, A., Dovesi, R., Kotomin, E.A.**
Electromechanical Properties of $Ba_{(1-x)}Sr_xTiO_3$Perovskite Solid Solutions from First-Principles Calculations
Journal of Physical Chemistry A, 121 (49), pp. 9409-9414.

4 **Nitiss, E., Tokmakovs, A., Pudzs, K., Busenbergs, J., Rutkis, M.**
All-organic electro-optic waveguide modulator comprising SU-8 and nonlinear optical polymer
Optics Express, 25 (25), pp. 31036-31044.

5 **Labrador-Páez, L., Pedroni, M., Smits, K., Speghini, A., Jaque, F., García-Solé, J., Jaque, D., Haro-González, P.**
Core–Shell Engineering to Enhance the Spectral Stability of Heterogeneous Luminescent Nanofluids
Particle and Particle Systems Characterization, 34 (12), art. no. 1700276, .

6 **Platonenko, A., Piskunov, S., Bocharov, D., Zhukovskii, Y.F., Evarestov, R.A., Bellucci, S.**
First-principles calculations on Fe-Pt nanoclusters of various morphologies
Scientific Reports, 7 (1), art. no. 10579, .

7 **Bocharov, D., Piskunov, S., Zhukovskii, Y.F., Spohr, E., D'yachkov, P.N.**
First principles modeling of 3d-metal doped three-layer fluorite-structured TiO_2 (4,4) nanotube to be used for photocatalytic hydrogen production
Vacuum, 146, pp. 562-569.

8 **Paris, P., Butikova, J., Laan, M., Aints, M., Hakola, A., Piip, K., Tufail, I., Veis, P.**
Detection of deuterium retention by LIBS at different background pressures
Physica Scripta, 2017 (T170), art. no. 014003, .

9 **Vlassov, S., Polyakov, B., Vahtrus, M., Mets, M., Antsov, M., Oras, S., Tarre, A., Arroval, T., LÕhmus, R., Aarik, J.**
Enhanced flexibility and electron-beam-controlled shape recovery in alumina-coated Au and Ag core-shell nanowires
Nanotechnology, 28 (50), art. no. 505707, .

10 **Fu, P., Wang, J., Jia, R., Bibi, S., Eglitis, R.I., Zhang, H.-X.**
Theoretical study on hydrogen storage capacity of expanded h-BN systems
Computational Materials Science, 139, pp. 335-340.

11 **Tumėnas, S., Mackonis, P., Nedzinskas, R., Trinkler, L., Berzina, B., Korsaks, V., Chang, L., Chou, M.M.C.**
Optical properties of lithium gallium oxide
Applied Surface Science, 421, pp. 837-842.

12 **Bakaev, A., Grigorev, P., Terentyev, D., Bakaeva, A., Zhurkin, E.E., Mastrikov, Yu.A.**
Trapping of hydrogen and helium at dislocations in tungsten: An ab initio study
Nuclear Fusion, 57 (12), art. no. 126040, .

13 **Vembris, A., Zarins, E., Kokars, V.**
Stimulated emission and optical properties of pyranyliden fragment containing compounds in PVK matrix

Optics and Laser Technology, 95, pp. 74-80.

14 **Yukhno, E.K., Bashkirov, L.A., Pershukevich, P.P., Kandidatova, I.N., Petrov, G.S., Mironova-Ulmane, N., Sarakovskis, A.**
Excitation and photoluminescence spectra of single- and non-single-phased phosphors based on $LaInO_3$ doped with Dy^{3+}, Ho^{3+}activators and Sb^{3+}probable sensitizer
Journal of Luminescence, 190, pp. 298-308.

15 **Zarins, A., Leys, O., Kizane, G., Supe, A., Baumane, L., Gonzalez, M., Correcher, V., Boronat, C., Zolotarjovs, A., Knitter, R.**
Behaviour of advanced tritium breeder pebbles under simultaneous action of accelerated electrons and high temperature
Fusion Engineering and Design, 121, pp. 167-173.

16 **Karitans, V., Lesina, N., Kassaliete, E., Svede, A., Laicane, I., Ekimane, L., Ozolins, M., Krumina, G.**
Measuring the refractive state of an eye based on the intensity of the retinal reflex
Journal of Modern Optics, 64 (17), pp. 1751-1761.

17 **Dutkiewicz, E.M., Suchanicz, J., Konieczny, K., Czaja, P., Kluczewska, K., Czternastek, H., Antonova, M., Sternberg, A.**
Electrical transport in lead-free $(Na_{0.5}Bi_{0.5})_{1-x}Sr_xTiO_3$ ceramics (x = 0, 0.01 and 0.02)
Phase Transitions, 90 (9), pp. 824-830.

18 **Dumbrajs, O., Kalis, H.**
Multimode time-dependent gyrotron equations for different time scales
Physics of Plasmas, 24 (9), art. no. 093111, .

19 **Zubkins, M., Kalendarev, R., Gabrusenoks, J., Plaude, A., Zitolo, A., Anspoks, A., Pudzs, K., Vilnis, K., Azens, A., Purans, J.**
Changes in structure and conduction type upon addition of Ir to ZnO thin films
Thin Solid Films, 636, pp. 694-701.

20 **Brezinsek, S., Coenen, J.W., Schwarz-Selinger, T., Schmid, K., Kirschner, A., Hakola, A., Tabares, F.L., Van Der Meiden, H.J., Mayoral, M.-L., Reinhart, M., Tsitrone, E., Ahlgren, T., Aints, M., Airila, M., Almaviva, S., Alves, E., Angot, T., Anita, V., Arredondo Parra, R., Aumayr, F., Balden, M., Bauer, J., Ben Yaala, M., Berger, B.M., Bisson, R., Björkas, C., Bogdanovic Radovic, I., Borodin, D., Bucalossi, J., Butikova, J., Butoi, B., Čadež, I., Caniello, R., Caneve, L., Cartry, G., Catarino, N., Čekada, M., Ciraolo, G., Ciupinski, L., Colao, F., Corre, Y., Costin, C., Craciunescu, T., Cremona, A., De Angeli, M., De Castro, A., Dejarnac, R., Dellasega, D., Dinca, P., Dittmar, T., Dobrea, C., Hansen, P., Drenik, A., Eich, T., Elgeti, S., Falie, D., Fedorczak, N., Ferro, Y., Fornal, T., Fortuna-Zalesna, E., Gao, L., Gasior, P., Gherendi, M., Ghezzi, F., Gosar, Ž., Greuner, H., Grigore, E., Grisolia, C., Groth, M., Gruca, M., Grzonka, J., Gunn, J.P., Hassouni, K., Heinola, K., Höschen, T., Huber, S., Jacob, W., Jepu, I., Jiang, X., Jogi, I., Kaiser, A., Karhunen, J., Kelemen, M., Köppen, M., Koslowski, H.R., Kreter, A., Kubkowska, M., Laan, M., Laguardia, L., Lahtinen, A., Lasa, A., Lazic, V., Lemahieu, N., Likonen, J., Linke, J., Litnovsky, A., Linsmeier, C., Loewenhoff, T., Lungu, C., Lungu, M., Maddaluno, G., Maier, H., Makkonen, T., Manhard, A., Marandet, Y., Markelj, S., Marot, L., Martin, C., Martin-Rojo, A.B., Martynova, Y., Mateus, R., Matveev, D., Mayer, M., Meisl, G., Mellet, N., Michau, A., Miettunen, J., Möller, S., Morgan, T.W., Mougenot, J., Mozetič, M., Nemanič, V., Neu, R., Nordlund, K., Oberkofler, M., Oyarzabal, E., Panjan, M., Pardanaud, C., Paris, P., Passoni, M., Pegourie, B., Pelicon, P., Petersson, P., Piip, K., Pintsuk, G., Pompilian, G.O., Popa, G., Porosnicu, C., Primc, G., Probst, M., Räisänen, J., Rasinski, M., Ratynskaia, S., Reiser, D., Ricci, D., Richou, M., Riesch, J., Riva, G., Rosinski, M., Roubin, P., Rubel, M., Ruset, C., Safi, E., Sergienko, G., Siketic, Z., Sima, A., Spilker, B., Stadlmayr, R., Steudel, I., Ström, P., Tadic, T., Tafalla, D., Tale, I., Terentyev, D., Terra, A., Tiron, V., Tiseanu, I., Tolias, P., Tskhakaya, D., Uccello, A., Unterberg, B., Uytdenhoven, I., Vassallo, E., Vavpetič, P., Veis, P., Velicu, I.L., Vernimmen, J.W.M., Voitkans, A., Von Toussaint, U., Weckmann, A., Wirtz, M., Založnik, A.,**

Zaplotnik, R.
Plasma-wall interaction studies within the EUROfusion consortium: Progress on plasma-facing components development and qualification
Nuclear Fusion, 57 (11), art. no. 116041, .

21 **Labrador-Páez, L., Jovanović, D.J., Marqués, M.I., Smits, K., Dolić, S.D., Jaque, F., Stanley, H.E., Dramićanin, M.D., García-Solé, J., Haro-González, P., Jaque, D.**
Unveiling Molecular Changes in Water by Small Luminescent Nanoparticles
Small, 13 (30), art. no. 1700968, .

22 **Ozolinsh, M., Paulins, P.**
Electro-optic control of photographic imaging quality through 'Smart Glass' windows in optics demonstrations
European Journal of Physics, 38 (5), art. no. 055704, .

23 **Bandura, A.V., Evarestov, R.A., Lukyanov, S.I., Piskunov, S., Zhukovskii, Y.F.**
Simulation of Young's moduli for hexagonal ZnO [0 0 0 1]-oriented nanowires: First principles and molecular mechanical calculations
Materials Research Express, 4 (8), art. no. 085014, .

24 **Ivanova, A., Tokmakov, A., Lebedeva, K., Roze, M., Kaulachs, I.**
Influence of the Preparation Method on Planar Perovskite $CH_3NH_3PbI_{3-x}Cl_x$ Solar Cell Performance and Hysteresis
Latvian Journal of Physics and Technical Sciences, 54 (4), pp. 58-68.

25 **Grehov, V., Kalnacs, J., Mishnev, A., Kundzins, K.**
Nitrogen Adsorption on Graphene Sponges Synthesized by Annealing a Mixture of Nickel and Carbon Powders
Latvian Journal of Physics and Technical Sciences, 54 (4), pp. 36-48.

26 **Pajuste, E., Kizane, G., Vitins, A., Igaune, I., Avotina, L., Zarins, R.**
Structure, tritium depth profile and desorption from ‘plasma-facing’ beryllium materials of ITER-Like-Wall at JET
Nuclear Materials and Energy, 12, pp. 642-647.

27 **Šutka, A., Döbelin, N., Joost, U., Smits, K., Kisand, V., Maiorov, M., Kooser, K., Kook, M., Duarte, R.F., Käämbre, T.**
Facile synthesis of magnetically separable $CoFe_2O_4/Ag_2O/Ag_2CO_3$ nanoheterostructures with high photocatalytic performance under visible light and enhanced stability against photodegradation
Journal of Environmental Chemical Engineering, 5 (4), pp. 3455-3462.

28 **Bellucci, S., Shunin, Y., Gopeyenko, V., Lobanova-Shunina, T., Burlutskaya, N., Zhukovskii, Y.**
Real time polymer nanocomposites-based physical nanosensors: Theory and modeling
Nanotechnology, 28 (35), art. no. 355502, .

29 **Yang, D.-C., Jia, R., Wang, Y., Kong, C.-P., Wang, J., Ma, Y., Eglitis, R.I., Zhang, H.-X.**
Novel Carbon Nanotubes Rolled from 6,6,12-Graphyne: Double Dirac Points in 1D Material
Journal of Physical Chemistry C, 121 (27), pp. 14835-14844.

30 **Merijs Meri, R., Zicans, J., Ābele, A., Ivanova, T., Kalniņš, M., Kundziņš, K.**
Modification of polyoxymethylene for increased thermal resistance
Polymer Engineering and Science, 57 (7), pp. 772-778.

31 **Kasatkin, P.E., Jäger, R., Härk, E., Teppor, P., Tallo, I., Joost, U., Šmits, K., Kanarbik, R., Lust, E.**
Fe-N/C catalysts for oxygen reduction based on silicon carbide derived carbon
Electrochemistry Communications, 80, pp. 33-38.

32 **Khutoryan, E.M., Idehara, T., Melnikova, M.M., Ryskin, N.M., Dumbrajs, O.**
Influence of Reflections on Frequency Tunability and Mode Competition in the Second-Harmonic THz Gyrotron

Journal of Infrared, Millimeter, and Terahertz Waves, 38 (7), pp. 824-837.

33 **Birks, E., Dunce, M., Peräntie, J., Hagberg, J., Sternberg, A.**
Direct and indirect determination of electrocaloric effect in $Na_{0.5}Bi_{0.5}TiO_3$
Journal of Applied Physics, 121 (22), art. no. 224102, .

34 **Ignatans, R., Dunce, M., Birks, E., Sternberg, A.**
Novel octahedral tilt system a+b+c+in $(1 - x)Na_{0.5}Bi_{0.5}TiO_{3-x}CdTiO_3$ solid solutions
Journal of Materials Science, 52 (12), pp. 7149-7157.

35 **Zhukovskii, Y.F., Piskunov, S., Lisovski, O., Bocharov, D., Evarestov, R.A.**
Doped 1D Nanostructures of Transition-metal Oxides: First-principles Evaluation of Photocatalytic Suitability
Israel Journal of Chemistry, 57 (6), pp. 461-476.

36 **Grigorjeva, L., Zolotarjovs, A., Sokovnin, S.Y., Millers, D., Smits, K., Il`ves, V.G.**
Radioluminescence, thermoluminescence and dosimetric properties of ZnO ceramics
Ceramics International, 43 (8), pp. 6187-6191.

37 **Ivanova, Z.G., Zavadil, J., Kostka, P., Djouama, T., Reinfelde, M.**
Photoluminescence properties of Er-doped Ge–In(Ga)–S glasses modified by caesium halides
Physica Status Solidi (B) Basic Research, 254 (6), art. no. e201600662, .

38 **Liepina, V., Millers, D., Smits, K.**
Tunneling luminescence in long lasting afterglow of $SrAl_2O_4$:Eu,Dy
Journal of Luminescence, 185, pp. 151-154.

39 **Timoshenko, J., Anspoks, A., Kalinko, A., Kuzmin, A.**
Thermal disorder and correlation effects in anti-perovskite-type copper nitride
Acta Materialia, 129, pp. 61-71.

40 **Gudeika, D., Bundulis, A., Mihailovs, I., Volyniuk, D., Rutkis, M., Grazulevicius, J.V.**
Donor and acceptor substituted triphenylamines exhibiting bipolar charge-transporting and NLO properties
Dyes and Pigments, 140, pp. 431-440.

41 **Zabels, R., Manika, I., Schwartz, K., Maniks, J., Dauletbekova, A., Grants, R., Baizhumanov, M., Zdorovets, M.**
Formation of dislocations and hardening of LiF under high-dose irradiation with 5–21 MeV ^{12}C ions
Applied Physics A: Materials Science and Processing, 123 (5), art. no. 320, .

42 **Bonny, G., Bakaev, A., Terentyev, D., Mastrikov, Yu.A.**
Interatomic potential to study plastic deformation in tungsten-rhenium alloys
Journal of Applied Physics, 121 (16), art. no. 165107,

43 **Trukhin, A.N., Antuzevics, A., Golant, K., Griscom, D.L.**
Luminescence of phosphorus doped silica glass
Journal of Non-Crystalline Solids, 462, pp. 10-16.

44 **Eglitis, R.I., Popov, A.I.**
Systematic trends in (001) surface ab initio calculations of ABO_3 perovskites
Journal of Saudi Chemical Society, . Article in Press.

45 **Krieke, G., Sarakovskis, A., Ignatans, R., Gabrusenoks, J.**
Phase transitions and upconversion luminescence in oxyfluoride glass ceramics containing $Ba_4Gd_3F_{17}$ nanocrystals
Journal of the European Ceramic Society, 37 (4), pp. 1713-1722.

46 **Popov, A.I., Kotomin, E.A., Maier, J.**
Analysis of self-trapped hole mobility in alkali halides and metal halides
Solid State Ionics, 302, pp. 3-6.

47 **Babin, V., Bohacek, P., Grigorjeva, L., Kučera, M., Nikl, M., Zazubovich, S., Zolotarjovs, A.**

Effect of Mg^{2+} ions co-doping on luminescence and defects formation processes in $Gd_3(Ga,Al)_5O_{12}$:Ce single crystals
Optical Materials, 66, pp. 48-58.

48 **Bujakiewicz-Koronska, R., Nalecz, D.M., Majcher, A.M., Juszynska-Galazka, E., Galazka, M., Vasylechko, L., Markiewicz, E., Majda, D., Kalvane, A., Koronski, K.**
Structural, magnetic, dielectric and mechanical properties of (Ba,Sr)MnO_3 ceramics
Journal of the European Ceramic Society, 37 (4), pp. 1477-1486.

49 **Revalde, G., Alnis, J., Nitišs, E., Blušs, K., Grundšteins, K.**
Cavity Ring-Down Spectroscopy measurements of Acetone concentration
Journal of Physics: Conference Series, 810 (1), art. no. 012036, .

50 **Gopejenko, A., Piskunov, S., Zhukovskii, Y.F.**
Ab initio modelling of the effects of varying Zr (Ti) concentrations on the atomic and electronic properties of stoichiometric PZT solid solutions
Computational and Theoretical Chemistry, 1104, pp. 56-60.

51 **Smits, K., Olsteins, D., Zolotarjovs, A., Laganovska, K., Millers, D., Ignatans, R., Grabis, J.**
Doped zirconia phase and luminescence dependence on the nature of charge compensation
Scientific Reports, 7, art. no. 44453,

52 **Kiselev, D.A., Neradovskaya, E.A., Turygin, A.P., Fedorovykh, V.V., Shikhova, V.A., Neradovskiy, M.M., Sternberg, A., Shur, V.Y., Kholkin, A.L.**
Effect of surface disorder on the domain structure of PLZT ceramics
Ferroelectrics, 509 (1), pp. 19-26.

53 **Skuja, L., Kajihara, K., Smits, K., Silins, A., Hosono, H.**
Luminescence and Raman Detection of Molecular Cl_2 and ClClO Molecules in Amorphous SiO_2 Matrix
Journal of Physical Chemistry C, 121 (9), pp. 5261-5266.

54 **Kallaev, S.N., Omarov, Z.M., Bakmaev, A.G., Mitarov, R.G., Reznichenko, L.A., Bormanis, K.**
Thermal properties of multiferroic $Bi_{1-x}Eu_xFeO_3$(x = 0–0.40) ceramics
Journal of Alloys and Compounds, 695, pp. 3044-3047.

55 **Burkhanov, A.I., Bormanis, K., Akbaeva, G.M., Zhirkov, A.V., Antonova, M., Livinsh, M.**
Relaxation of polarization in $(K_{0.5}Na_{0.}5)(Nb_{0.93}Sb_{0.0}7)O_3$ ferroelectric ceramics modified by $BaTiO_3$
Ferroelectrics, 508 (1), pp. 93-99.

56 **Dimza, V., Popov, A.I., Lāce, L., Kundzins, M., Kundzins, K., Antonova, M., Livins, M.**
Effects of Mn doping on dielectric properties of ferroelectric relaxor PLZT ceramics
Current Applied Physics, 17 (2), pp. 169-173.

57 **Butanovs, E., Kuzmin, A., Butikova, J., Vlassov, S., Polyakov, B.**
Synthesis and characterization of ZnO/ZnS/MoS_2 core-shell nanowires
Journal of Crystal Growth, 459, pp. 100-104.

58 **Leonarska, A., Kądziołka-Gaweł, M., Szeremeta, A.Z., Bujakiewicz-Korońska, R., Kalvane, A., Molak, A.**
Electric relaxation and Mn^{3+}/Mn^{4+} charge transfer in Fe-doped $Bi_{12}MnO_{20}$–$BiMn_2O_5$ structural self-composite
Journal of Materials Science, 52 (4), pp. 2222-2231.

59 **Bonny, G., Bakaev, A., Terentyev, D., Mastrikov, Y.A.**
Elastic properties of the sigma W-Re phase: A first principles investigation
Scripta Materialia, 128, pp. 45-48.

60 **Pudzs, K., Vembris, A., Rutkis, M., Woodward, S.**
Thin Film Organic Thermoelectric Generator Based on Tetrathiotetracene
Advanced Electronic Materials, 3 (2), art. no. 1600429,

61 **Yukhno, E.K., Bashkirov, L.A., Pershukevich, P.P., Kandidatova, I.N., Mironova-Ulmane, N., Sarakovskis, A.**
Excitation and emission spectra of $LaInO_3$ -based solid solutions doped with Sm^{3+}, Sb^{3+}
Journal of Luminescence, 182, pp. 123-129.

62 **Pierzga, A., Błachowski, A., Komędera, K., Ruebenbauer, K., Kalvane, A., Bujakiewicz-Korońska, R.**
Orientation of the electric field gradient and ellipticity of the magnetic cycloid in multiferroic $BiFeO_3$
Philosophical Magazine, 97 (3), pp. 168-174.

63 **Bormanis, K., Burkhanov, A.I., Smeltere, I., Antonova, M., Kalvane, A., Garbarz-Glos, B.**
Dielectric properties of potassium–sodium niobate ceramics at low frequencies
Phase Transitions, 90 (1), pp. 54-59.

64 **Bujakiewicz-Koronska, R., Vasylechko, L., Markiewicz, E., Nalecz, D.M., Kalvane, A.**
X-ray and dielectric characterization of Co doped tetragonal $BaTiO_3$ ceramics
Phase Transitions, 90 (1), pp. 78-85.

65 **Kemere, M., Sperga, J., Rogulis, U., Krieke, G., Grube, J.**
Luminescence properties of Eu, RE^{3+} (RE = Dy, Sm, Tb) co-doped oxyfluoride glasses and glass–ceramics
Journal of Luminescence, 181, pp. 25-30.

66 **Paiders, M., Gruduls, A., Kalnina, L., Valucka, S., Dimanta, I., Kleperis, J., Nikolajeva, V.**
Biogas and hydrogen production from glycerol by enterobacter aerogenes and anaerobic microbial communities
Agronomy Research, 15 (1), pp. 256-269.

67 **Nitiss, E., Tokmakov, A.**
Determination of refractive index of submicron-thick films using resonance shift in a four-layer slab waveguide
Proceedings of SPIE - The International Society for Optical Engineering, 10242, art. no. 102420X, .

68 **Krieke, G., Sarakovskis, A., Springis, M.**
Upconversion luminescence of a transparent glass ceramics with hexagonal $Na(Gd,Lu)F_4$ nanocrystals
Journal of Alloys and Compounds, 694, pp. 952-958.

69 **Nitiss, E.**
Evaluation of performance of a hybrid electro-optic directional coupler and a Mach-Zehnder switch
Journal of Nanophotonics, 11 (1), art. no. 016013,

70 **Bundulis, A., Mihailovs, I., Nitiss, E., Busenbergs, J., Rutkis, M.**
Determination of Kerr and two-photon absorption coefficients of indandione derivatives
Proceedings of SPIE - The International Society for Optical Engineering, 10228, art. no. 1022804, .

71 **Linina, E., Bundulis, A., Nitiss, E., Rutkis, M.**
Poling dynamics of an EO active material using parallel-plate electrodes
Proceedings of SPIE - The International Society for Optical Engineering, 10228, art. no. 1022816, .

72 **Kuzovkov, V.N., Kotomin, E.A., Popov, A.I.**
Kinetics of dimer F_2 type center annealing in MgF_2 crystals
Nuclear Instruments and Methods in Physics Research, Section B: Beam Interactions with Materials and Atoms, . Article in Press.

73 **Mozolevskis, G., Nitiss, E., Medvids, A.**
Electric breakdown of dielectric thin films for high-voltage display applications
Proceedings of SPIE - The International Society for Optical Engineering, 10022, art. no. 100222S.

74 **Lisovski, O., Piskunov, S., Zhukovskii, Y.F., Bocharov, D.**
Quantum chemical simulations of titanium dioxide nanotubes used for photocatalytic water splitting
Journal of Surface Investigation, 11 (1), pp. 78-86.

75 **Kotomin, E.A., Merkle, R., Mastrikov, Yu.A., Kuklja, M.M., Maier, J.**
The effect of (La,Sr)MnO_3 cathode surface termination on its electronic structure
ECS Transactions, 77 (10), pp. 67-73.

76 **Mozolevskis, G., Sekacis, I., Nitiss, E., Medvids, A., Rutkis, M.**
Dielectric breakdown of fast switching LCD shutters
Proceedings of SPIE - The International Society for Optical Engineering, 10126, art. no. 1012607, .

77 **Miao, L., Jia, R., Wang, Y., Kong, C.-P., Wang, J., Eglitis, R.I., Zhang, H.-X.**
Certain doping concentrations caused half-metallic graphene
Journal of Saudi Chemical Society, 21 (1), pp. 111-117.

78 **Cipa, J., Kizane, G., Supe, A., Zolotarjovs, A., Zarins, A., Baumane, L.**
Luminescence of x-ray induced radiation defects in modified lithium orthosilicate pebbles with additions of titanium dioxide [Rentgeno spindulių sukeltų defektų liuminescencija modifikuotuose ličio ortosilikato rutuliukuose su titano dioksido priedais]
Energetika, 63 (3), pp. 113-120.

79 **Rozenberga-Voska, L., Grabis, J., Zolotarjovs, A.**
Synthesis of Eu^{2+} and Dy^{3+} doped strontium aluminates and their properties
Key Engineering Materials, 721 KEM, pp. 311-315.

80 **Evarestov, R.A., Gryaznov, D., Arrigoni, M., Kotomin, E.A., Chesnokov, A., Maier, J.**
Use of site symmetry in supercell models of defective crystals: Polarons in CeO_2
Physical Chemistry Chemical Physics, 19 (12), pp. 8340-8348.

81 **Bocharov, D., Chollet, M., Krack, M., Bertsch, J., Grolimund, D., Martin, M., Kuzmin, A., Purans, J., Kotomin, E.**
Analysis of the U L_3-edge X-ray absorption spectra in UO_2 using molecular dynamics simulations
Progress in Nuclear Energy, 94, pp. 187-193.

82 **Lisovski, O., Kenmoe, S., Piskunov, S., Bocharov, D., Zhukovskii, Y.F., Spohr, E.**
Validation of a constrained 2D slab model for water adsorption simulation on 1D periodic TiO2nanotubes
Computational Condensed Matter, . Article in Press.

83 **Kokina, I., Jahundoviča, I., Mickeviča, I., Jermaļonoka, M., Strautiņš, J., Popovs, S., Ogurcovs, A., Sledevskis, E., Polyakov, B., Gerbreders, V.**
Target Transportation of Auxin on Mesoporous Au/SiO_2 Nanoparticles as a Method for Somaclonal Variation Increasing in Flax (L. usitatissimum L.)
Journal of Nanomaterials, 2017, art. no. 7143269 .

84 **Lesnicenoks, P., Zemitis, J., Grinberga, L., Chikvaidze, G., Kleperis, J., Urbonavičius, M., Tučkute, S., Milčius, D.**
Modified graphene sheet stacks for hydrogen binding
Medziagotyra, 23 (1), pp. 3-5.

85 **Evarestov, R.A., Piskunov, S., Zhukovskii, Y.F.**
Site symmetry approach in the supercell model of carbon-doped ZnO bulk
Chemical Physics Letters, 682, pp. 91-95

86 **Evarestov, R.A., Platonenko, A., Gryaznov, D., Zhukovskii, Y.F., Kotomin, E.A.**
First-principles calculations of oxygen interstitials in corundum: A site symmetry approach
Physical Chemistry Chemical Physics, 19 (37), pp. 25245-25251.

87 **Mironovs, V., Lisicins, M., Onufrijevs, P., Muktepavela, F., Medvids, A.**

Hardening of steel perforated tape by Nd:YAG laser
Key Engineering Materials, 721 KEM, pp. 456-460.

88 **Joost, U., Šutka, A., Visnapuu, M., Tamm, A., Lembinen, M., Antsov, M., Utt, K., Smits, K., Nõmmiste, E., Kisand, V.**
Colorimetric gas detection by the varying thickness of a thin film of ultrasmall PTSA-coated TiO_2 nanoparticles on a Si substrate
Beilstein Journal of Nanotechnology, 8 (1), pp. 229-236.

89 **Heifets, E., Kotomin, E.A., Bagaturyants, A.A., Maier, J.**
Thermodynamic stability of stoichiometric $LaFeO_3$ and $BiFeO_3$: A hybrid DFT study
Physical Chemistry Chemical Physics, 19 (5), pp. 3738-3755.

90 **Lushchik, A., Dolgov, S., Feldbach, E., Pareja, R., Popov, A.I., Shablonin, E., Seeman, V.**
Creation and thermal annealing of structural defects in neutron-irradiated $MgAl_2O_4$ single crystals
Nuclear Instruments and Methods in Physics Research, Section B: Beam Interactions with Materials and Atoms, . Article in Press.

91 **Shirmane, L., Feldmann, C., Pankratov, V.**
Comparing the luminescence processes of YVO_4:Eu and core-shell YVO_4@YF_3 nanocrystals with bulk-YVO_4:Eu
Physica B: Condensed Matter, 504, pp. 80-85

92 **Traskovskis, K., Bundulis, A., Mihailovs, I.**
Unusual response to environmental polarity in a nonlinear-optical benzylidene-type chromophore containing a 1,3-bis(dicyanomethylidene)indane acceptor fragment
Physical Chemistry Chemical Physics, 20 (1), pp. 404-413.

93 **Trinkler, L., Trukhin, A., Berzina, B., Korsaks, V., Ščajev, P., Nedzinskas, R., Tumėnas, S., Chou, M.M.C., Chang, L., Li, C.-A.**
Luminescence properties of $LiGaO_2$ crystal
Optical Materials, 69, pp. 449-459.

94 **Czaja, P., Suchanicz, J., Kluczewska, K., Sitko, D., Dutkiewicz, E.M., Konieczny, K., Węgrzyn, A., Antonova, M., Sternberg, A.**
Influence of uniaxial pressure on dielectric properties of (1-x)$Na_{0.5}Bi_{0.5}TiO_{3-x}SrTiO_3$ for x = 0.01, 0.04, and 0.1 ceramics
Proceedings of the Estonian Academy of Sciences, Volume 66, Issue 4, 20 December 2017, Pages 396-402

95 **Bormanis, K., Burkhanov, A.I., Sternberg, A., Zhirkov, A.V., Antonova, M., Kalvane, A., Ignatans, R.**
Polarization and acoustic properties of barium-modified lead-free potassium-sodium niobate ceramics [Baariumiga modifitseeritud pliivaba KNN-keraamika polarisatsioon ja akustilised omadused]
Proceedings of the Estonian Academy of Sciences, 66 (4), pp. 372-376.

96 **Bormanis, K., Gorev, M.G., Flerov, I.N., Sternberg, A., Lace, L., Ignatans, R., Kalvane, A., Antonova, M.**
Behaviour of thermal expansion of (1-x)$Pb(Ni_{1/3}Nb_{2/3})O_{3-x}PbTiO_3$ solid solutions | [(1-x)$Pb(Ni_{1/3}Nb_{2/3})O_{3-x}PbTiO_3$ tahke lahuse soojuspaisumine]
Proceedings of the Estonian Academy of Sciences, 66 (4), pp. 363-371.

97 **Antuzevics, A., Kemere, M., Krieke, G., Ignatans, R.**
Electron paramagnetic resonance and photoluminescence investigation of europium local structure in oxyfluoride glass ceramics containing SrF_2 nanocrystals
Optical Materials, 72, pp. 749-755.

98 **Skuja, L., Kajihara, K., Smits, K., Alps, K., Silins, A., Teteris, J.**
Luminescence properties of chlorine molecules in glassy SiO_2 and optical fibre waveguides

Proceedings of the Estonian Academy of Sciences, 66 (4), pp.455-461

99 **Trukhin, A.N.**
Luminescence of α-quartz crystal and silica glass under excitation of excimer lasers ArF (193 nm), KrF (248 nm)
Journal of Luminescence, 188, pp. 524-528.

100 **Kjapsna, A., Dimitrocenko, L., Tale, I., Trukhin, A., Ignatans, R., Grants, R.**
Characterization of crystalline structure and morphology of Ga_2O_3 thin film grown by MOCVD technique
Key Engineering Materials, 721 KEM, pp. 253-257.

101 **Lesnicenoks, P., Berzina, A., Lukosevics, I., Grinberga, L., Jekabsons, L., Kleperis, J., Knite, M., Taurins, G.**
Complex multilayer carbon structures for green energetics
Proceedings of the Estonian Academy of Sciences (2017) Volume: 66 Issue: 4 Pages: 403-408.

102 **Knoks, A., Kleperis, J., Grinberga, L.**
Raman spectral identification of phase distribution in anodic titanium dioxide coating
Proceedings of the Estonian Academy of Sciences, Volume: 66 Issue: 4 Pages: 422-429.

103 **Soto, C., García-Rosales, C., Echeberria, J., Martínez-Esnaola, J.M., Hernández, T., Malo, M., Platacis, E., Muktepavela, F.**
SiC-based sandwich material for Flow Channel Inserts in DCLL blankets: Manufacturing, characterization, corrosion tests
Fusion Engineering and Design, 124, pp. 958-963.

104 **Arrigoni, M., Kotomin, E.A., Maier, J.**
First-principles Study of Perovskite Ultrathin Films: Stability and Confinement Effects
Israel Journal of Chemistry, 57 (6), pp. 509-521.

105 **Ozolinsh, M., Paulins, P.**
Electro-optic control of photographic imaging quality through 'Smart Glass' windows in optics demonstrations
European Journal of Physics 38(5), 055704.

Theses

Doctor Theses

No.	Author	Title	Supervisor	Degree
1.	**Liāna Širmane**	Nanostrukturētu komplekso oksīdu luminoforu vakuuma ultravioletās ierosmes spektroskopija *Vacuum Ultraviolet Excitation Spectroscopy of Nanostructured Complex Oxide Phosphors*	Dr. Phys. **Vladimirs Pankratovs**	Dr. Phys.
2.	**Andris Antuzevičs**	S-stāvokļu retzemju jonu lokālā struktūra fluorīdos un oksifluorīdu stikla keramikās *Local Structure of S-State Rare Earth Ions in Fluorides and Oxyfluoride Glass Ceramics*	Prof., Dr. Hab. Phys. **Uldis Rogulis**	Dr. Phys.
3.	**Gatis Mozoļevskis**	*Dielectric Breakdown of High Voltage Liquid Crystal Displays*	Dr. Phys. **Mārtiņš Rutkis**	Dr. Eng.

M.Sc. Theses

No.	Author	Mark	Title	Supervisor
1.	**Inga Jonāne**	10	Nanokristāliskā itrija oksīda lokālās struktūras pētījumi *Study of nanocrystalline yttrium oxide local structure*	**Aleksejs Kuzmins,** Dr. Phys., LU CFI vad. pētnieks
2.	**Gatis Priedītis**	8	Eiropija jonu luminiscence nātrija alumosilikāta-stroncija fluorīda stikla keramikās *Luminiscence of europium ions in sodium aluminosilicate-strontium fluoride glass ceramics*	**Meldra Ķemere,** M.Sc. Phys, LU CFI pētniece **Uldis Rogulis,** Dr.hab.Phys., LU professor
3.	**Arturs**	9	ODS tērauda izejmateriālu lokālās struktūra	**Andris Anspoks,**

	Cintiņš		analīze izmantojot Ti un Y K-malas rentgenabsorbcijas spektroskopiju. *ODS steel raw material local structure analysis using Ti and Y K-edge X-ray absorption spectroscopy.*	Dr. Phys., LU CFI vad. pētnieks
4.	**Ieva Grauduma**	7	Nanostrukturēta titāna dioksīda izmantošana oglekļa dioksīda reducēšanai *Nanostructured titania for reduction of carbon dioxide*	**Jānis Kleperis,** Dr. Phys., LU CFI vad. pētnieks
5.	**Katrina Loganovska**	8	Luminiscences kinētikas mērījumu iekārta *Equipment for Luminescence Kinetics Measurements*	**Māris Zeltiņš** Fakultāte: Elektronikas un telekomunikāciju fakultāte, RTU **Krišjānis Šmits** Dr.Phys., LU CFI vad. pētnieks
6.	**Ivita Bite**	9	Jūras vides kvalitātes kritēriju un pārtikas risku robežvērtību izstrāde, pamatojoties uz metālisko elementu (Cd, Cu, Hg, Pb un Zn) uzkrāšanās tendencēm Baltijas jūras un Rīgas līča zivīs *Quality criteria of marine environmental and food hazard threshold development, based on accumulation tendencies of metallic elements (Cd, Cu, Hg, Pb and Zn) in fishes of the Baltic Sea and the Gulf of Riga*	**Rita Poikāne** Fakultāte: Ķīmijas fakultāte, LU
7.	**Staņislavs Ložkins**	8	Protonus vadoša polimēra un polianilīna nanopulvera kompozītmateriāla sintēze un pētījumi pielietojumiem ūdeņraža enerģētikā *Synthesis and research of proton conductive polymer and polyaniline nanopowder composite material for applications in hydrogen energetics.*	**Julija Hodakovsk**a, Dr. Phys., LU CFI vad. pētnieks **Remo Merijs Meri**, Dr. Sc. Ing., RTU profesors
8.	**Maksims**	17.3	Photonics and optoelectronic devices	**Dr. Mattieu**

	Sokolovs	(no 20.0)	(maģistra grāds tika piešķirts pēc MSc kursu pabeigšanas divas Skotijas universitātēs: Sent Andrews un Heriot Watt)	**Rayer**

B.Sc. Theses

No.	Author	Mark	Title	Supervisor
1.	**Poļina Krivolapova**	7	Metālisko un heterogēno nanodaļiņu iegūšana ar lāzerablacijas metodi šķidrumā *Synthesis of pure and heterogeneous metallic nanoparticles using laser ablation in liquid*	**Jeļena Butikova,** Dr. Phys., LU CFI vad. pētniece
2.	**Ginta Kazuša**	7	ZnO plāno kārtiņu izgatavošana pie zemām temperatūrām ar reaktīvo magnetrono izputināšanas metodi un to raksturošana *Deposition and characterization of ZnO thin films deposited by reactive magnetron sputtering at low temperatures*	**Mārtiņš Zubkins,** Mag. Phys., LU CFI zinātniskais asistents
3.	**Dāgs Olšteins**	9	Caurspīdīgu nanostrukturētu keramiku iegūšana un izpēte *Sintering and research of transparent nanostructured ceramics*	**Krišjānis Šmits,** Dr. Phys., LU CFI vad. pētnieks
4.	**Līga Bikše**	9	Redzes asuma ietekme uz šaušanas rezultātiem *Effect of visual acuity on shooting results*	**Gatis Ikaunieks,** Dr.phys., pētnieks